Neuropharmacology 111 (2016) 266–282

Contents lists available at ScienceDirect

Neuropharmacology

journal homepage: www.elsevier.com/locate/neuropharm

Selective and differential interactions of BNN27, a novel C17-spiroepoxy steroid derivative, with TrkA receptors, regulating neuronal survival and differentiation

Iosif Pediaditakis [a, b], Paschalis Efstathopoulos [a, b], Kyriakos C. Prousis [c], Maria Zervou [c], Juan Carlos Arévalo [d], Vasileia I. Alexaki [e], Vassiliki Nikoletopoulou [b], Efthymia Karagianni [f], Constantinos Potamitis [c], Nektarios Tavernarakis [b], Triantafyllos Chavakis [e], Andrew N. Margioris [f], Maria Venihaki [f], Theodora Calogeropoulou [c], Ioannis Charalampopoulos [a, *], Achille Gravanis [a, b, **]

[a] Department of Pharmacology, School of Medicine, University of Crete, Heraklion, Greece
[b] Institute of Molecular Biology & Biotechnology, Foundation of Research & Technology-Hellas (IMBB-FORTH), Heraklion, Greece
[c] Institute of Biology, Medicinal Chemistry & Biotechnology, National Hellenic Research Foundation, Athens, Greece
[d] Department of Cell Biology and Pathology, Instituto de Neurociencias de Castilla y León (INCyL), Universidad de Salamanca, Salamanca, Spain
[e] Department of Internal Medicine III, Technical University Dresden, Dresden, Germany
[f] Department of Clinical Chemistry, School of Medicine, University of Crete, Heraklion, Greece

ARTICLE INFO

Article history:
Received 18 February 2016
Received in revised form
11 August 2016
Accepted 7 September 2016
Available online 9 September 2016

Keywords:
Neurotrophins
Nerve growth factor (NGF)
TrkA
Neurodegeneration
Neurotrophin receptors signaling
Neuronal apoptosis
Steroid
STD NMR
Molecular modeling

ABSTRACT

Nerve growth factor (NGF) holds a pivotal role in brain development and maintenance, been also involved in the pathophysiology of neurodegenerative diseases. Here, we provide evidence that a novel C17-spiroepoxy steroid derivative, BNN27, specifically interacts with and activates the TrkA receptor of NGF, inducing phosphorylation of TrkA tyrosine residues and down-stream neuronal survival-related kinase signaling. Additionally, BNN27 potentiates the efficacy of low levels of NGF, by facilitating its binding to the TrkA receptors and differentially inducing fast return of internalized TrkA receptors into neuronal cell membranes. Furthermore, BNN27 synergizes with NGF in promoting axonal outgrowth, effectively rescues from apoptosis NGF-dependent and TrkA positive sympathetic and sensory neurons, *in vitro, ex vivo* and *in vivo* in NGF null mice. Interestingly, BNN27 does not possess the hyperalgesic properties of NGF. BNN27 represents a lead molecule for the development of neuroprotective TrkA receptor agonists, with potential therapeutic applications in neurodegenerative diseases and in brain trauma.

1. Introduction

NGF, the first described neurotrophin, controls the development and phenotypic maintenance of sympathetic and sensory neurons in the peripheral nervous system (PNS) by preventing cell death, as well as the functional integrity of cholinergic neurons within the

Abbreviations: NGF, nerve growth factor; BDNF, brain-derived neurotrophic factor; NT-3, neurotrophin-3; CYP17, cytochrome P450 17-hydroxylase/17,20-lyase; DHEA, dehydroepiandrosterone; ADIOL, 5-androsten-3β,17β—diol; BNN27, C17-spiroepoxy analog of DHEA; PEG-BNN27, polyethylene glycol amino resin-supported BNN27; SCG, superior cervical ganglia; DRG, dorsal root ganglia; GAPDH, glyceraldehyde-3-phosphate dehydrogenase; HEK293, human embryonic kidney cell line 293; CHO, Chinese Hamster Ovary cell line; PC12, pheochromacytoma cells; Trk, tropomyosin related kinase; ERK, Extracellular signal-regulated kinase; JNK, c-Jun N-terminal kinase; ECD, Extracellular Domain; MβCD, methyl-β-cyclodextran; STD NMR, saturation transfer difference nuclear magnetic resonance; MD, molecular dynamics; ip, intraperitoneal; AD, Alzheimer's disease.

* Corresponding author. Department of Pharmacology, School of Medicine, University of Crete, Heraklion, Greece.
** Corresponding author. Department of Pharmacology, School of Medicine, University of Crete, Heraklion, Greece & Institute of Molecular Biology Biotechnology, Foundation of Research and Technology-Hellas (IMBB-FORTH), Heraklion, Greece.
E-mail addresses: charalampn@uoc.gr (I. Charalampopoulos), gravania@uoc.gr (A. Gravanis).

http://dx.doi.org/10.1016/j.neuropharm.2016.09.007
0028-3908/

central nervous system (CNS) (Bibel and Barde, 2000). The mature form of NGF derives from the proteolytic cleavage of its precursor protein, proNGF, and exerts its effects via a specific and of high affinity binding to the TrkA receptor (Kaplan and Miller, 2000). NGF also binds to and activates $p75^{NTR}$, albeit with lower affinity compared to its precursor molecule, proNGF (Teng et al., 2005). The hallmark of the biological action of NGF in the nervous system is its potent anti-apoptotic and neuroprotective effects via its binding to the TrkA receptor which activates transcription factors CREB and NFκB, controlling the anti-apoptotic Bcl-2 proteins (Yuan and Yankner, 2000).

In CNS, NGF plays a pivotal role in the survival and function of cholinergic neurons of the basal forebrain affected in Alzheimer's disease (Rossner et al., 1998; Calissano et al., 2010). It was recently reported that NGF has a beneficial effect on β-amyloid-mediated neurotoxicity and tau-phosphorylation, two major factors in the pathophysiology of Alzheimer's disease (Matrone et al., 2008; Zhang et al., 2010). However, the clinical use of NGF is severely compromised by its limited ability to penetrate the blood-brain barrier (BBB), its pharmacokinetic properties and its poor stability in serum. To bypass these limitations, intra-cerebro-ventricular (icv) infusion of NGF has been attempted in patients with Alzheimer's disease (AD), albeit with limited success and hyperalgesic, pain-related secondary effects described for NGF (Eriksdotter Jonhagen et al., 1998). Currently, therapeutic options that are less invasive are being explored including NGF gene therapy (Tuszynski et al., 2005, 2015), and the intranasal delivery of recombinant NGF (Covaceuszach et al., 2009; Tian et al., 2012).

We have recently reported that neurosteroid dehydroepiandrosterone (DHEA), produced by neurons, glia and the adrenal cortex (Charalampopoulos et al., 2008), exerts part of its neuroprotective properties (Charalampopoulos et al., 2004) via binding at nanomolar (nM) concentrations to and activation of both NGF receptors TrkA and $p75^{NTR}$ (Lazaridis et al., 2011). Binding of DHEA to TrkA receptors results in its tyrosine phosphorylation, activation of the transcription factors CREB and NFκB and the transcriptional control of the production of anti-apoptotic protein Bcl-2 (Charalampopoulos et al., 2004; Lazaridis et al., 2011). It is worth noticing that DHEA binds to all mammalian and invertebrate Trk receptors, although with affinity lower by two orders of magnitude compared to that of the polypeptidic neurotrophins (Pediaditakis et al., 2015). DHEA is a multifaceted agent, interacting with steroid and neurotransmitter receptors, and acting as an endogenous precursor for the biosynthesis of androgens, estrogens and their metabolites (Charalampopoulos et al., 2008). We have recently synthesized several synthetic C17-spiro derivatives of DHEA, such as BNN27 [(R)-3β,21-dihydroxy-17*R*,20-epoxy-5-pregnene], that are devoid of any estrogenic or androgenic activities and are unable to bind to and activate steroid hormone receptors (Calogeropoulou et al., 2009). Interestingly, BNN27 was shown to protect the PC12 cell line against serum deprivation induced apoptosis at nanomolar concentrations (Calogeropoulou et al., 2009).

The aim of the present study was 1) to examine the efficacy of BNN27 as a NGF synthetic substitute in protecting against apoptosis NGF sensitive TrkA receptor-expressing sensory and sympathetic neurons *in vitro*, *ex vivo* and *in vivo* in NGF null mice, 2) to test its potency to intervene in the neuronal pathways conveying hyperalgesia *in vivo*, 3) to define the ability of BNN27 to interact with and activate TrkA receptors and the exact post-receptor cellular mechanisms by which it affects NGF-sensitive cell signaling related to neuronal cell fate and axonal growth. Several physicochemical methods (NMR and pull-down assays with recombinant TrkA) were also used to clarify the molecular interactions of BNN27 with TrkA receptors. Based on our findings we propose BNN27 as an effective lead molecule for the development of BBB-permeable, neuroprotective, synthetic NGF small analogs, with potential therapeutic applications in neurodegenerative diseases and in brain trauma.

2. Materials and methods

2.1. Plasmids, antibodies, proteins

Plasmids expressing TrkA, TrkB, TrkC and shRNAs against TrkA were previously described (Lazaridis et al., 2011; Pediaditakis et al., 2015). ERβ plasmid was kindly provided from Dr. E.R. Levin (Irvine VA, Long Beach). The $TrkA^{C302S}$ construct was previously described (Arevalo et al., 2000). Normal expression of all constructs was verified by immunoblotting. The origin and exact dilutions for all

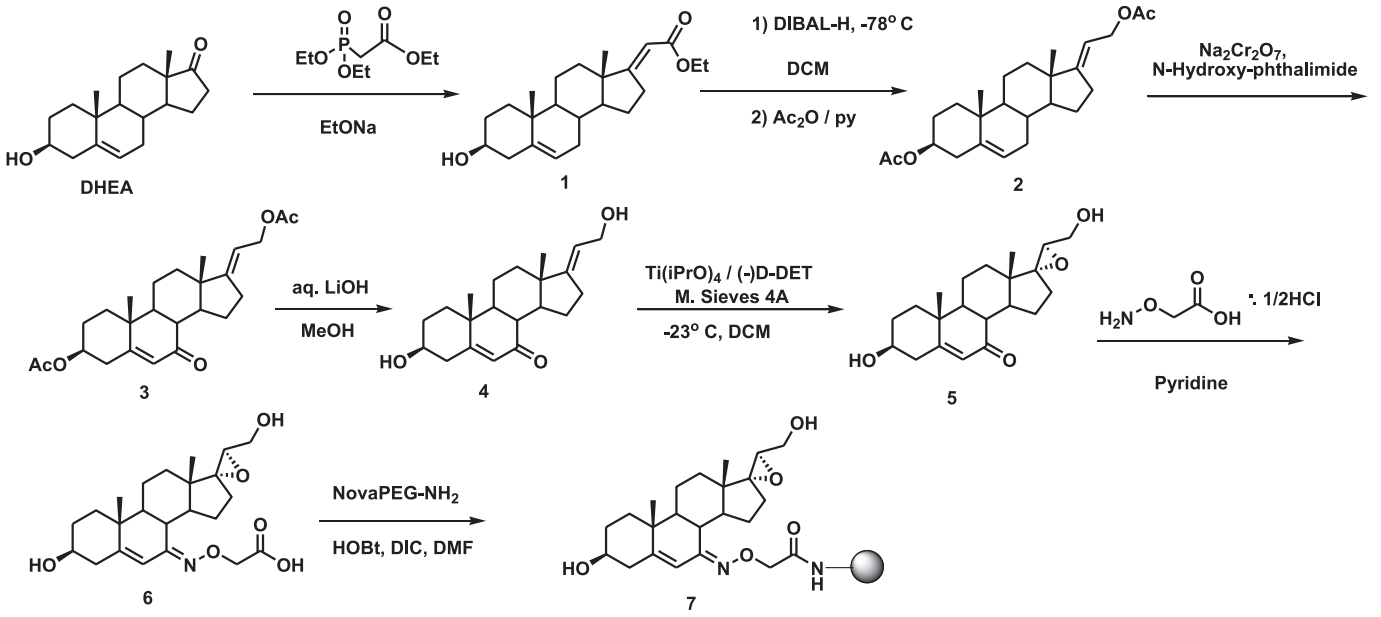

Scheme 1..

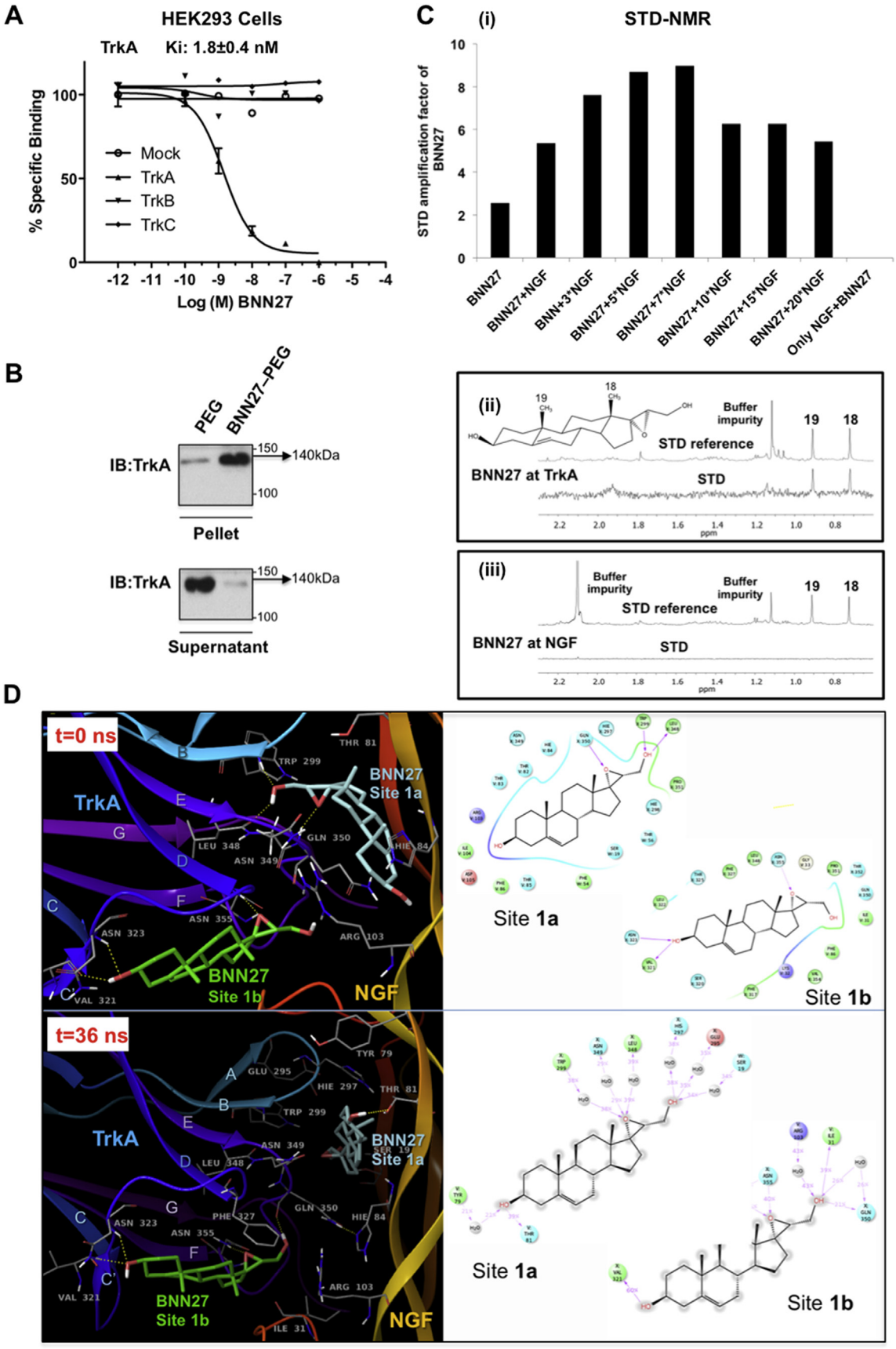
A
HEK293 Cells
TrkA Ki: 1.8±0.4 nM
% Specific Binding
Mock
TrkA
TrkB
TrkC
Log (M) BNN27
B
PEG
BNN27–PEG
IB:TrkA
140kDa
Pellet
IB:TrkA
140kDa
Supernatant
C
(i)
STD-NMR
STD amplification factor of BNN27
BNN27
BNN27+NGF
BNN+3'NGF
BNN27+5'NGF
BNN27+7'NGF
BNN27+10'NGF
BNN27+15'NGF
BNN27+20'NGF
Only NGF+BNN27
(ii)
Buffer impurity
STD reference
BNN27 at TrkA
STD
(iii)
Buffer impurity
Buffer impurity
STD reference
BNN27 at NGF
STD
ppm
D
t=0 ns
TrkA
BNN27 Site 1a
BNN27 Site 1b
NGF
t=36 ns
TrkA
BNN27 Site 1a
BNN27 Site 1b
NGF
Site 1a
Site 1b
Site 1a
Site 1b

antibodies and growth factors are described in Supplementary Information.

2.2. Cell lines and transfection

PC12, HEK293, CHO, BV-2 cells were obtained from LGC Promochem and cultured under specific conditions for each cell line. HEK293, CHO and BV-2 cells were grown in DMEM medium containing 10% fetal bovine serum (charcoal-stripped for removing endogenous steroids), 100 units/ml penicillin, and 0.1 mg/ml streptomycin, at 5% CO_2 and 37 °C. PC12 were grown in RPMI 1640 containing 2 mM L-glutamine, 15 mM HEPES, 100 units/ml penicillin, 0.1 mg/ml streptomycin, and 10% horse serum, 5% fetal calf serum (both charcoal-stripped for removing endogenous steroids) at 5% CO_2 and 37 °C. Cells were transfected with TurboFect (Fermentas) or Lipofectamin 2000 (Invitrogen) according to manufacturers' instructions. Transfected cells were typically used on the 2nd day after transfection.

2.3. Primary neuronal cultures and immunocytochemistry

Superior cervical ganglia (SCG) and Dorsal root ganglia (DRG) were dissected from newborn (P0–P1) rat pups and then dissociated in 0.25% trypsin (Cat. No. 15090; Gibco) for 30 min at 37 °C. For NGF withdrawal experiments, SCG neurons after dissociation were cultured for 7 d in RPMI culture medium 1640 containing 3% fetal bovine serum (FBS), 100 units/ml penicillin, 0.1 mg/ml streptomycin, 100 ng/ml NGF and the antimitotic agent FdU, in order to obtain an almost pure (>90%) neuronal culture. SCG neurons were subsequently deprived of NGF for 12 h and exposed for 15 min to either NGF (100 ng/ml) or BNN27 (100 nM) in the presence of an anti-NGF antibody ((1 μg/m) (Cat. No. AB1526SP; Millipore) to block endogenously produced NGF. For assessment of survival, SCG neurons were washed twice with NGF free medium and cultured for 48 h in medium lacking NGF and containing BNN27 (100 nM) and anti-NGF antibody (1 μg/m). At the end of the treatment period, neurons were immunostained against neurofilament protein using NF200kD antibody and TUNEL assay was performed (Cat. No. 11684795910; Roche) in order to stain apoptotic neurons. For assessment of axonal growth, sensory neurons of dissociated DRG neurons were incubated for 24 h with NGF (20 ng/ml) at the time of plating in the absence or the presence of BNN27 (100 nM) and stained with an antibody against NF200kD. To measure neurite length of isolated sensory neurons, random neurons (at least 50 clearly separated neurons selected per dish) were imaged using a Zeiss Axiovision microscope with an AxioCam HRC digital camera and analyzed with Axiovision software.

2.4. In vivo detection of apoptosis

ngf$^{+/-}$ mice (White et al., 1996) were obtained from the Jackson Laboratory and maintained on C57BL/6 background. They were kept in the Animal House of the Institute of Molecular Biology and Biotechnology (IMBB-FORTH, Heraklion, Greece). All research activities strictly adhered to the EU adopted Directive 2010/63/EU on the protection of animals used for scientific purposes. Mice heterozygous for the NGF gene disruption were interbred and the pregnant mothers were treated daily with an intra-peritoneal injection of BNN27 (3 mg/day) or vehicle (4.5% ethanol in 0.9% saline) starting from the third day after gestation until day E13.5. At the end of the treatment mothers were euthanized by cervical dislocation and embryos were collected and fixed overnight. The embryo samples were sectioned (16 μm) in a freezing microtome and mounted onto Superfrost plus slides (Menzel-Glaser J1800AMNZ). Slides were post fixed for 10 min in cold acetone and left to dry for 10 min at room temperature. They were then washed in PB 0.1 M, and incubated for 1 h at RT with 5% horse serum in TBS-T 0.1%. After this slides were incubated with primary antibodies (Cleaved Caspase-3 antibody and NF200kD), in TBS-T 0.1% with 1% horse serum overnight at 4 °C, followed by 3 washes with TBS and incubation with secondary antibodies (anti-rabbit Alexa Fluor 488 and anti-chicken Alexa Fluor 546, respectively) for 1 h at RT in TBS-T 0.1%. Sections were washed with TBS again and coverslipped with antifade reagent (InVitrogen) and visualized using confocal microscopy. In order to quantify apoptotic neurons in embryos, caspase-3 positive cells inside the area of the DRG were counted in 12–14 sections being 160 μM apart from one another across most of the rostrocaudal extent of the spinal cord and the mean of apoptotic cells per sections was estimated.

2.5. Immunoprecipitation and immunoblotting

48 h after transfection, CHO cells were starved from serum for 4–6 h and stimulated with BNN27 (100 nM) or the appropriate neurotrophin (100 ng/ml) for the indicated times. Cells were suspended in lysis buffer (50 mM Tris-HCl, 0.15 M NaCl, 1% Triton-X100, pH 7.4) supplemented with protease inhibitors (1 mM PMSF and 1 g/ml aprotinin). Lysates were pre-cleared for 1 h with protein G-plus Agarose beads (Cat No. sc-2002; Santa Cruz) and immunoprecipitated with the appropriate antibody overnight at 4 °C. Protein G-plus agarose beads were incubated with the lysates for 4 h at 4 °C with gentle shaking. Beads were collected by centrifugation, washed four times with lysis buffer and resuspended in SDS loading buffer. Concerning the PC12 cells, after 24 h of transfection PC12 cells were starved from serum for 12 h and stimulated with BNN27 (100 nM) or NGF (100 ng/ml) for indicated times. Cells were then rinsed with ice-cold PBS and solubilized in SDS lysis buffer. Immunoblots were developed using the ECL Western Blotting Kit (Thermo Scientific) and exposed to Kodak X-Omat AR films. Image analysis and quantification of band intensities were done with ImageQuant (GE Healthcare).

2.6. Flow cytometry-based apoptosis detection

PC12 cells were cultured in 12-well plates, and 24 h later they were transfected with the shRNAs for TrkA receptor. 24 h later the medium was aspirated and replaced either with complete medium (serum supplemented) or serum free medium in the absence or the

Fig. 1. BNN27 specifically binds to TrkA receptor. (**A**) Competition binding assays of [^{3}H]-DHEA in the presence of increasing concentrations of BNN27 using membranes isolated from HEK293 cells transfected with cDNAs of TrkA or TrkB or TrkC receptors. Ki represents the mean ± SEM, n = 6 experiments. Right panels depict efficacy of transfection as assessed by Western blots. (**B**) Covalently linked BNN27 to polyethylene glycol amino resin pulled down TrkA shown by Western blot analysis. (**C**) (i) STD-NMR revealed the interaction between BNN27 and TrkA, further amplified upon NGF additions. The null STD amplification suggested no interaction of BNN27 with NGF alone. (ii-iii) ^{1}H STD-NMR and the corresponding STD-reference spectra. The binding of BNN27 at TrkA is evidenced by the presence of BNN27 methyls (18, 19) at the STD spectra; their absence in the case of NGF indicates the lack of BNN27-NGF interaction. (**D**) MD simulations (50 ns) of the 2TrkA:2NGF-BNN27 Modeled Complex. (Upper panel) Initial state with BNN27 bound at TrkA sites **1a** and **1b**. At the 2D interaction diagrams, TrkA residues are marked as X and NGF monomers residues as V and W. BNN27 at **1a** disrupts H-bonds between Gln350 (TrkA) - His84 (NGF) and Asn349(TrkA) - Arg103(NGF). (Lower panel) A representative 3D frame of the MD simulation (water-mediated interactions are omitted) along with the 2D diagrams depicting the stabilized BNN27 interactions. During the simulation, the ligand harbored at site **1a** shifts its 3-OH upwards to favor H-bonding with NGF (Thr81 or Tyr79 via water), reestablishing the contact between Gln350(TrkA) - His84(NGF). At site **1b**, BNN27 bridges TrkA and NGF through the developed H-bonds as illustrated.

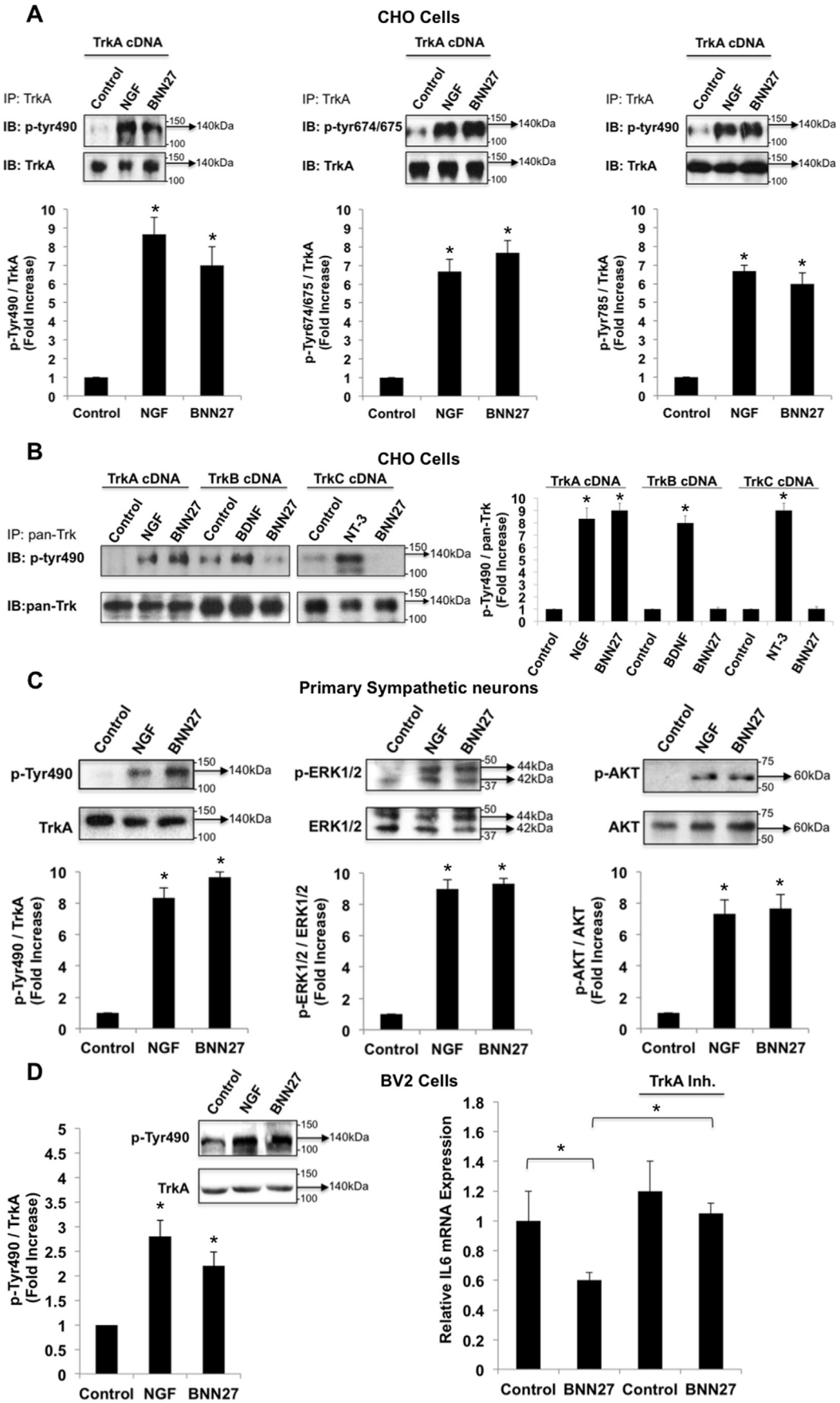
A
CHO Cells
TrkA cDNA
Control
NGF
BNN27
IP: TrkA
IB: p-tyr490
IB: TrkA
IB: p-tyr674/675
150
100
140kDa
p-Tyr490 / TrkA (Fold Increase)
p-Tyr674/675 / TrkA (Fold Increase)
p-Tyr785 / TrkA (Fold Increase)
B
CHO Cells
TrkA cDNA
TrkB cDNA
TrkC cDNA
BDNF
NT-3
IP: pan-Trk
IB: p-tyr490
IB:pan-Trk
p-Tyr490 / pan-Trk (Fold Increase)
C
Primary Sympathetic neurons
p-Tyr490
TrkA
p-ERK1/2
ERK1/2
p-AKT
AKT
44kDa
42kDa
60kDa
p-Tyr490 / TrkA (Fold Increase)
p-ERK1/2 / ERK1/2 (Fold Increase)
p-AKT / AKT (Fold Increase)
D
BV2 Cells
TrkA Inh.
Relative IL6 mRNA Expression

presence of BNN27 at 100 nM. Apoptosis was quantified 24 h later. PC12 cells at a concentration of 1×10^{-6} were fixed and permeabilized by re-suspending in 100 μl of Cytofix/Cytoperm (BD Biosciences) buffer on ice for 30 min, followed by the addition of 0.5 ml of BD Perm/Wash buffer (1×) (BD Biosciences). After washing and centrifuging (300 × g for 5 min), the cells were stained using the Cleaved Caspase-3 antibody for 30 min on ice. Afterwards, the cells were washed, centrifuged (300 × g for 5 min) and the secondary antibody (anti-rabbit Alexa Fluor 488) was added for 30 min on ice. Following washing and centrifuging, the cells were re-suspended in 0.5 ml BD Perm/Wash buffer (1×) and analyzed in a Beckton-Dickinson FACSArray apparatus and the CELL-Quest software (Beckton-Dickinson, Franklin Lakes, NJ).

2.7. Binding assays

HEK293 cells were transfected with the cDNA expression plasmids coding for TrkA, TrkB, TrkC or ERβ. Western blot inserts show the efficacy of transfection. Crude membrane fractions were isolated by differential centrifugation at 2500 g (10 min at 4 °C to remove unbroken cells and nuclei) and 100,000 g (1 h, at 4 °C). A constant concentration of [^{3}H]-DHEA (5 nM) was incubated with increasing concentrations of BNN27 (from 10^{-12} to 10^{-6} M) in a final volume of 100 μl. For the competitive binding assay, increasing concentrations of BNN27 (from 10^{-12} to 10^{-6} M) or estradiol (from 10^{-12} to 10^{-6} M) were incubated with cytosol (~250 μg protein) in the presence of 4 nm of [^{3}H] 17β-estradiol for 18 h at 4 °C. Bound [^{3}H] estradiol was measured in scintillation fluid (SigmaFluor, Sigma) in a scintillation counter (Perkin Elmer, Foster City, CA) with 60% efficiency for tritium.

2.8. Pull down assays

Recombinant Rat Trk A/Fc Chimera (source) was incubated overnight at 4 °C with the NovaPEG amino resin alone or conjugated with BNN27. Beads were collected by centrifugation, washed four times with lysis buffer, and re-suspended in SDS loading buffer. Proteins were separated by SDS/PAGE, followed by immunoblotting with specific antibodies.

2.8.1. Synthesis of BNN27 conjugated to NovaPEG amino resin (Scheme 1)

BNN27 conjugated to NovaPEG amino resin was synthesized according to Scheme 1. Briefly, Horner-Emmons reaction of DHEA with triethylphosphonoacetate afforded compound **1** which in turn, was treated with DIBAL-H to afford the acetylated allylic alcohol **2** after treatment with acetic anhydride in pyridine. Allylic oxidation at position C7 using sodium dichromate dehydrate and *N*-hydroxyphthalimide afforded the 7-keto derivative **3**. Hydrolysis of the acetate esters using LiOH in methanol gave the diol **4**. Sharpless epoxidation of the allylic alcohol at C17 using *D*-(−)-diethyl tartrate and titanium (IV) isopropoxide afforded the 17*R*,20*R* spiro-epoxide **5**. Reaction of the C7-ketone of compound **5** with *O*-(carboxymethyl)hydroxylamine hemihydrochloride gave the corresponding 7-(*O*-carboxymethyl)oxime **6**, which in turn reacted with NovaPEG amino resin after activation with HOBt and DIC to afford the immobilized BNN-27 (**7**).

The experimental details are described in the Supplementary Information.

2.9. STD-NMR experiments

The recombinant Rat TrkA/Fc chimera containing the rat TrkA extracellular domain was purchased by R&D Systems, Inc. NGF (NGF 2.5S, mouse) was purchased by Millipore. D_2O 99.9% from Euriso-Top was used for the PBS buffer.

NMR samples were prepared in Shigemi NMR tubes using D_2O (99.9%) PBS buffer, pD = 7.4. The solutions of TrkA/BNN27 and NGF/BNN27 were prepared using a protein concentration of 0.6 μM and a ligand concentration of 60 μM, resulting in protein:ligand ratio of 1:100. Successive additions of NGF were applied to the solution of TrkA/BNN27 at 1:1 up to 1:20 molar ratios of TrkA:NGF. In the case of the solution TrkA/BNN27, the addition of NGF reached a molar ratio of 1:30 (TrkA:NGF). NMR spectra were acquired on an Agilent (Varian) 600 MHz NMR spectrometer at 25 °C using a 1H{13C/15N} 5 mm PFG Automatable Triple Resonance probe. Experiments were run using the pulse sequences provided by the Varian BioPack library. The ^{1}H STD NMR experiments were recorded with a spectral width of 12019 Hz, 8192 complex data points, and 4000 scans. Selective on-resonance irradiation frequency was set to −0.94 ppm for TrkA, and −0.94 ppm for NGF and the off-resonance irradiation frequency was applied at 30 ppm. The saturation scheme consisted of a train of 50 ms Gauss-shaped pulses separated by a 0.1 ms delay with total duration of 2.5 s. Subtraction of the on-resonance and off-resonance spectra was performed internally via phase cycling. Water suppression was achieved with excitation sculpting. Control spectra were recorded under identical conditions on samples containing only BNN27 to test for artifacts. The STD amplification factor was obtained by averaging the respective STD amplification factors for the C18 and C19 methyl group peaks of BNN27 in the studied solutions. The STD amplification factor is calculated according to the formula:

$$\text{STD amplification factor} = (I_0 - I_{sat})/I_0 \times \text{ligand excess}$$

where (I_0-I_{sat}) corresponds to the STD intensity of one resonance signal and I_0 is the corresponding intensity obtained from the off resonance spectrum or reference spectrum.

2.10. Molecular modeling studies

The crystal complex 2TrkA:2NGF (pdb: 1www) was used for the molecular modeling studies.

Binding site prediction was performed by applying SiteMap algorithm, Schrödinger Suite 2013, in both monomers of TrkA-d5 of the crystal complex after removing the NGF homodimer. The predicted sites were characterized as druggable based on Sitescore and Dscore functions (values > 0.80 and around 1.00 respectively).

Molecular Dynamics Simulations were performed with Schrodinger Desmond 3.8 using the OPLS 2005 force field. Each modeled system was solvated in an orthorhombic simulation buffer box of size 20 Å in each direction with TIP4P water molecules and the

Fig. 2. BNN27 activates TrkA signaling in neuronal and glial cells. (**A**) BNN27 induces phosphorylation of tyrosine residues Y490, Y674/675 and Y785 of TrkA receptors. CHO cells were transfected with the plasmid cDNA of TrkA. Transfectants were then exposed for 15 min, to NGF (100 ng/ml) or BNN27 (100 nM). (**B**) BNN27 specifically induces phosphorylation of TrkA but not of TrkB or TrkC. CHO cells were transfected with the plasmid cDNA of TrkA, TrkB, or TrkC. Transfectants were then exposed for 15 min, to NGF (100 ng/ml) or BDNF (100 ng/ml) or NT3 (100 ng/ml) or BNN27 (100 nM). (**C**) BNN27 induces TrkA tyrosine phosphorylation (*p*-Tyr490), affecting downstream signaling pathways of MAPKs (ERK1/2) and AKT, in NGF-dependent rat sympathetic neurons in culture, after 15 min of exposure. (**D**) BNN27 induces *p*-Tyr490 on mouse microglia BV2 cells. (Left panel) BV2 cells treated for 15 min with NGF (100 ng/ml) or BNN27 (100 nM). (Right panel) Real-time PCR for IL6 mRNA, on total RNA isolated from BV2 cells incubated for 4 h with BNN27 (100 nM) in plus/minus 1 μM TrkA Inhibitor. Lysates were subjected to Western blot analysis using specific antibodies against the indicated proteins. Relative density was calculated by densitometric scanning of phosphorylated signals normalized to total levels. Results are representative of three experiments (mean ± SEM, n = 3 experiments, $^*P < 0.05$).

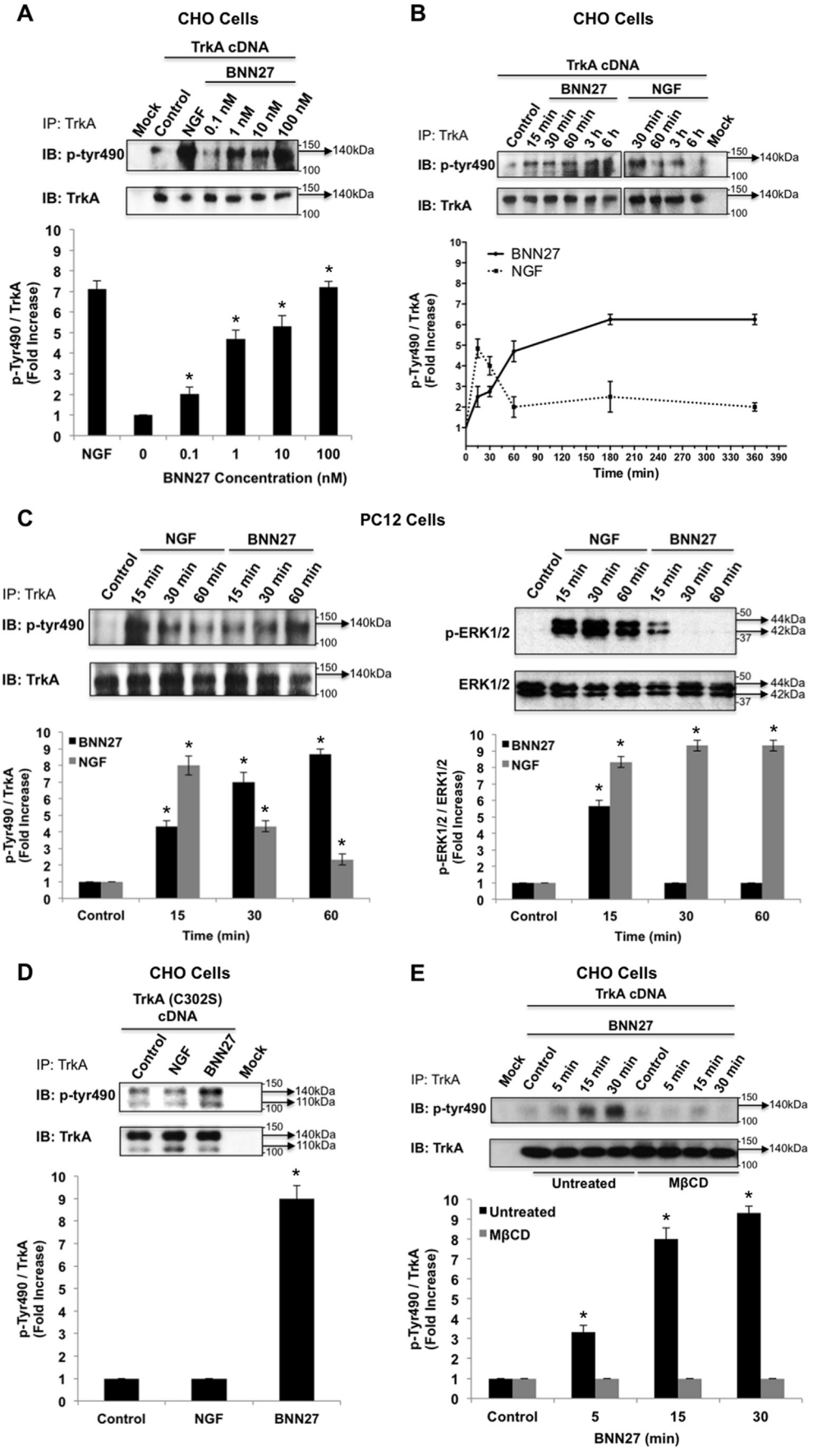
A
CHO Cells
TrkA cDNA
BNN27
Mock
Control
NGF
0.1 nM
1 nM
10 nM
100 nM
IP: TrkA
IB: p-tyr490
IB: TrkA
150
100
140kDa
p-Tyr490 / TrkA (Fold Increase)
NGF
0
0.1
1
10
100
BNN27 Concentration (nM)
B
CHO Cells
TrkA cDNA
BNN27
NGF
Control
15 min
30 min
60 min
3 h
6 h
30 min
60 min
3 h
6 h
Mock
IP: TrkA
IB: p-tyr490
IB: TrkA
BNN27
NGF
p-Tyr490 / TrkA (Fold Increase)
Time (min)
C
PC12 Cells
NGF
BNN27
Control
15 min
30 min
60 min
IP: TrkA
IB: p-tyr490
IB: TrkA
p-ERK1/2
ERK1/2
50
37
44kDa
42kDa
p-Tyr490 / TrkA (Fold Increase)
p-ERK1/2 / ERK1/2 (Fold Increase)
Control
15
30
60
Time (min)
D
CHO Cells
TrkA (C302S) cDNA
Control
NGF
BNN27
Mock
IP: TrkA
IB: p-tyr490
IB: TrkA
140kDa
110kDa
p-Tyr490 / TrkA (Fold Increase)
Control
NGF
BNN27
E
CHO Cells
TrkA cDNA
BNN27
Mock
Control
5 min
15 min
30 min
Control
5 min
15 min
30 min
IP: TrkA
IB: p-tyr490
IB: TrkA
Untreated
MβCD
p-Tyr490 / TrkA (Fold Increase)
Control
5
15
30
BNN27 (min)

appropriate number of sodium counter-ions, randomly distributed in the aqueous phase. Before the production run, the model system was relaxed through a series of minimizations and short MD simulations were performed using Desmond default values. Production runs were performed in the NPT ensemble at 300 K and 1.01325 bar with periodic boundary conditions. The RESPA integrator was used with time step 2 fs for bonded and short-range interactions and 6 fs for long-range interactions. During equilibration the Berendsen thermostat and barostat were applied with coupling time constants of 100 ps and 1000 ps, respectively. The cutoff distance for the Coulombic interactions was set to 9 Å, while the long-range Coulombic interactions were calculated using the smooth Particle Mesh Ewald (PME) method with a tolerance of 1e-09.

MD simulations of BNN27 and DHEA at the TrkA monomers were run for 20 ns and 50 ns. In each case four molecules were placed in the vicinity of each TrkA monomer at an average distance of 5–6 Å from the predicted binding sites (i.e**. 1a, 1b, 2** and **3)**.

MD simulations of BNN27 at the 2TrkA:2NGF complex were run for 50 ns. The modeled system was constructed by merging: i) TrkA with two BNN27 molecules bound at sites **1a** and **1b,** ii) the NGF homodimer along with the second TrkA monomer, obtained from the crystal structure and, iii) two more BNN27 molecules placed near the entrance of sites **1a** and **1b** of the second TrkA monomer (Supplementary Information).

2.11. Quantitative real-time reverse transcription-PCR

Total RNA of microglial cells was extracted, DNase treated, reverse transcribed and analyzed by real-time PCR with the following primers for detecting IL6 mRNA: F 5′-CAAAGCCAGAGTCCTTCAGAG-3′; R 5′-TGGTCCTTAGCCACTCCTTC-3″.

2.12. Cholesterol depletion and lipid rafts fractionation

CHO cells were transfected with the TrkA cDNA plasmid and pretreated with 10 mM methyl-β-cyclodextrin (MβCD) for 20 min. Fractionation of detergent resistant membranes by sucrose gradient was performed in HEK293 cells as previously described (Nikoletopoulou et al., 2010). Twenty fractions were collected, of which the two uppermost (fractions 1 and 2) were devoid of proteins and hence omitted from further analysis. Fractions 3–11 were analyzed by Western blot on 10% acrylamide gels and blotted on nitrocellulose membranes following standard procedures. Membranes were then analyzed for flotillin-1 (a marker of lipid raft microdomains) and TrkA. Fractions 12–20 were not Flotilin-1 positive (data not shown).

2.13. Surface biotinylation assays

PC12 cells were biotinylated as described (Yu et al., 2011) and then treated with NGF (100 ng/ml) or BNN27 (100 nM) for 5, 15 and 30 min. Biotin from non-internalized proteins was removed using reducing conditions as described (Yu et al., 2011). Cell lysates were prepared, biotinylated proteins were subjected to precipitation with neutroavidin beads and western blot analyses were performed with the corresponding antibodies.

2.14. Pain analysis

To determine the effect of BNN27 in thermal hyperalgesia in mice under basal conditions, we used the Hargreaves test (Hargreaves et al., 1988). Measurements were taken 30 min following (1 mg) intraplantar or (3 mg) intraperitoneal (i.p.) injection of BNN27. The control groups were given intraplantar injections of either the vehicle (DMSO) or (1 μg) NGF.

2.15. Statistics

All results are reported as the mean ± SEM. Comparison of 2 groups was performed using an unpaired *t*-test. For multiple group comparisons, ANOVA followed by Bonferroni's post-hoc correction was applied. Statistical analyses were performed using GraphPrism, version 6 (GraphPad Software Inc.). A *P* value of less than 0.05 was considered significant.

2.16. Study approval

All mouse experiments were approved by the Ethics Committees of the University of Crete, School of Medicine and FORTH.

3. Results

3.1. BNN27 specifically interacts with TrkA receptor

Saturation and competition binding assays with [^{3}H]-DHEA have shown that DHEA binds to all Trk receptors with Ki at nanomolar concentrations (Lazaridis et al., 2011; Pediaditakis et al., 2015). Based on these findings, we designed and carried out heterologous competition assays using [^{3}H]-DHEA, cold BNN27 and membranes isolated from HEK293 cells, transfected either with an empty vector (negative control) or with a specific TrkA vector (Fig. 1A). BNN27, the synthetic C17-spiroepoxy-derivative of DHEA, effectively displaced the bound [^{3}H]-DHEA on membranes isolated from HEK293^{TrkA} transfectants (Ki of 1.8 ± 0.4 nM, n = 6) (Fig. 1A). In contrast, BNN27 did not displace the binding of [^{3}H]-DHEA to membranes isolated from HEK293 cells transfected with the cDNAs of TrkB or the TrkC receptors (Fig. 1A). As in the case of DHEA, BNN27 was ineffective in displacing binding of iodinated NGF to TrkA receptors, suggesting different binding sites for this molecule (data not shown).

DHEA and its first metabolite ADIOL (5-androsten-3β,17β-diol) were shown to bind to Estrogen Receptor beta (ERβ) (Ki: 200 nM and 1 nM respectively) (Miller et al., 2013). However, BNN27 was unable to displace binding of [^{3}H]-estradiol to cytosolic preparations, isolated from HEK293 cells transfected with the cDNA of ERβ receptors (Supplementary Fig. S1). It is of note that ADIOL was ineffective in displacing binding of [^{3}H]-DHEA to membranes isolated from HEK293^{TrkA} transfectants (data not shown), suggesting that small structural changes in these steroid molecules are responsible for important differences in their interaction with the

Fig. 3. BNN27 triggers TrkA activation in a different manner than that of NGF. (**A**) BNN27 induces TrkA phosphorylation at tyrosine 490 in a dose-dependent manner. CHO cells were transfected with the plasmid cDNA of TrkA. Transfectants were then exposed for 15 min to NGF (100 ng/ml) or BNN27 (0.1 nM, 1 nM, 10 nM, 100 nM). (**B**) BNN27 induces TrkA phosphorylation at tyrosine 490 in a time-dependent manner. CHO cells were transfected with the plasmid cDNA of TrkA. Transfectants were then exposed at the indicated time points to NGF (100 ng/ml) or BNN27 (100 nM). (**C**) BNN27 induces *p*-Tyr490, affecting ERK1/2 kinases in a time-dependent manner. PC12 cells were treated with either NGF (100 ng/ml) or BNN27 (100 nM) at the indicated time points. (**D**) CHO cells were transfected with TrkA mutant receptor (C302S) lacking NGF extracellular binding domain. Transfectants were exposed for 15 min to NGF (100 ng/ml) or BNN27 (100 nM). (**E**) Cholesterol depletion of membranes limited BNN27-induced TrkA phosphorylation. CHO cells were transfected with a TrkA plasmid and treated with 10 mM methyl-β-cyclodextrin (MβCD). After 20 min, cells were exposed to BNN27 (100 nM) at the indicated time points. Lysates were immunoprecipitated with TrkA-specific antibodies, and then immunoblotted with *p*-Tyr490. Relative density was calculated by densitometric scanning of phosphorylated signals normalized to total levels. All results are representative of three experiments (mean ± SEM, n = 3, $^*P < 0.05$).

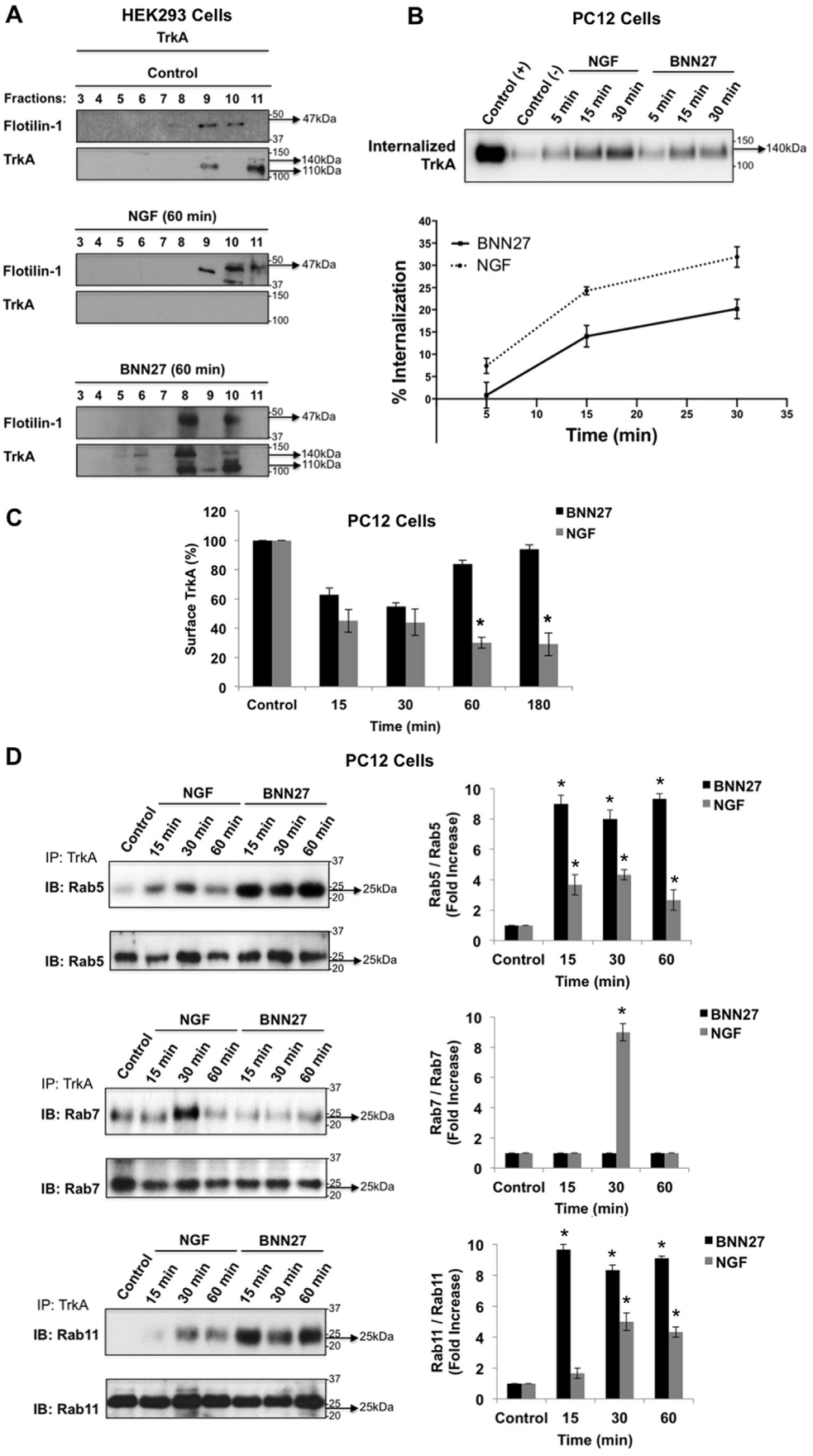
A
HEK293 Cells
TrkA
Control
Fractions: 3 4 5 6 7 8 9 10 11
Flotilin-1
TrkA
47kDa
140kDa
110kDa
NGF (60 min)
BNN27 (60 min)
B
PC12 Cells
Control (+)
Control (-)
NGF
BNN27
5 min
15 min
30 min
Internalized TrkA
140kDa
% Internalization
Time (min)
C
PC12 Cells
Surface TrkA (%)
Control
15
30
60
180
D
PC12 Cells
IP: TrkA
IB: Rab5
IB: Rab7
IB: Rab11
25kDa
Rab5 / Rab5 (Fold Increase)
Rab7 / Rab7 (Fold Increase)
Rab11 / Rab11 (Fold Increase)

TrkA receptors.

3.2. Immobilized BNN27 pulls down recombinant TrkA receptor

To assess the potential direct, physical interaction of BNN27 with recombinant TrkA receptor, we covalently linked BNN27-7-(*O*-carboxymethyl)oxime (BNN27-7-CMO) to polyethylene glycol amino resin (NovaPEG amino resin) (see Supplementary Information: Synthesis Materials and Methods) and tested the ability of immobilized BNN27 to pull down recombinant TrkA proteins. Precipitation experiments and western blot analysis of precipitates with specific antibodies against TrkA showed that immobilized BNN27 effectively precipitated recombinant TrkA proteins (Fig. 1B).

3.3. Saturation transfer difference (STD) NMR spectroscopy reveals the interaction of BNN27 with recombinant TrkA receptor: in silico binding studies

The application of saturation transfer difference (STD) NMR spectroscopy enabled the monitoring of the interactions between BNN27 and recombinant TrkA in the absence or presence of the neurotrophin NGF [Fig. 1C **(i)**]. The concept of this method relies on the magnetization transfer from the effectively saturated protein to the bound ligand (Mayer and Meyer, 1999; Meyer and Peters, 2003). The presence of the ligand resonance lines in the acquired STD-NMR spectrum signals the binding event. STD-NMR revealed the binding of BNN27 at the TrkA receptor as depicted by the presence of BNN27 resonance peaks (19Me and 18Me) in the respective spectra [Fig. 1C **(ii)**]. On the other hand, the lack of the corresponding resonances in the NGF solution [Fig. 1C **(iii)**] indicates that BNN27 does not interact with the NGF in the absence of TrkA. The STD amplification factor is a measure of the ligand:protein interaction. Interestingly, the addition of NGF to the TrkA solutions induces an increase of the BNN27 STD amplification factor indicating an enhancement of BNN27 binding [Fig. 1C **(i)**]. This upward trend reaches a peak at a molar ratio of TrkA: NGF in the order of 1:(5–7), followed by a slight decay and a plateau formation for molar ratios above 1:15. Further additions of NGF to the solution TrkA/BNN27 up to a molar ratio of 1:30 (TrkA:NGF) confirmed this trend to a greater extent (data not shown).

Since domain-5 of the extracellular part of TrkA is crucial in NGF binding and the STD-NMR data indicate the involvement of NGF in the TrkA:BNN27 interaction, we utilized the 2TrkA:2NGF heterodimeric complex (Wiesmann et al., 1999) for our *in silico* studies. Initially, we investigated the interactions of BNN27 with TrkA-d5 monomer. Three potential druggable binding sites were identified at the protein surface (Supplementary Fig. S2); among them, subsites **1a** and **1b** located at TrkA:NGF interface were probed by MD simulations as the most potent to harbor BNN27 (Supplementary Fig. S3). Docking studies by (Scarpi et al., 2012) have also proposed site **1b** as a binding groove of MT2, a small molecule agonist of TrkA with NGF-mimetic activity. Our simulations have shown that TrkA residues crucial for the interaction with NGF were also in contact with BNN27 (Supplementary Fig. S3). Thus, it was tempting to investigate the interaction of BNN27 with the 2TrkA:2NGF heterodimeric complex. As MD simulations revealed, albeit BNN27 initially anchored at TrkA sites **1a** and **1b** disrupt protein-protein interactions at TrkA:NGF interfacial region, in the course of the simulation, they develop stable interactions bridging TrkA and NGF heterodimer (Fig. 1D).

Furthermore, MD simulations investigated the interactions of DHEA with TrkA-d5. DHEA showed affinity for site **1b** but it develops fewer contacts as compared to BNN27 (Supplementary Fig. S4). It seems that the extended pharmacophore of BNN27 (epoxide and 21-OH functionalities) bearing both H-bond donor and acceptor properties is crucial for the accommodation in the pocket, enabling the ligand to cling to the protein using both its polar edges.

3.4. BNN27 activates TrkA signaling in neuronal and glial cells

It is well established that the auto-phosphorylation of tyrosine residue 490 following binding to NGF is the initial and sine *qua non* step in TrkA receptor activation and signaling (Kaplan and Miller, 2000). The effect of BNN27 on tyrosine-490 TrkA phosphorylation was confirmed by using TrkA-negative CHO cells transfected with TrkA receptor cDNA (Fig. 2A). BNN27 was furthermore mimicking NGF in inducing the phosphorylation of TrkA at tyrosine residues 674/675 and 785 in CHO^{TrkA} transfectants (Fig. 2A). However, BNN27 did not induce the phosphorylation of tyrosine residue 490 in CHO cells transfected with the cDNAs of TrkB or TrkC receptors (Fig. 2B). This set of data is in agreement with our competition binding data, showing no affinity of BNN27 for these two receptors (Fig. 1A). Induction of TrkA phosphorylation at tyrosine residue 490 by BNN27 was further validated with immunofluorescence experiments in PC12 cells endogenously expressing the TrkA receptors. BNN27 and NGF clearly increased the intracellular staining of tyrosine-490-phospho-TrkA, in contrast to E2 and ADIOL where no activation was observed, confirming our data from TrkA binding competition assays (data not shown). We therefore examined the ability of BNN27 to induce the phosphorylation of TrkA at tyrosine residue 490 on NGF-dependent primary sympathetic neurons. Western blot analysis using specific antibodies against TrkA or tyrosine-490-phospho-TrkA showed that 100 nM of BNN27 was effective in mimicking NGF at 100 ng/ml. Indeed, NGF induced the phosphorylation of TrkA at tyrosine residue 490, activating also the two TrkA down-stream pro-survival kinases ERK1/2 and AKT following an exposure of 15 min (Fig. 2C).

In addition to its effect on neuronal cells, 100 nM BNN27 induced the phosphorylation of TrkA at tyrosine residue 490 of TrkA-positive BV2 mouse glial cells in culture (Fig. 2D, left panel), functionally decreasing the mRNA levels of interleukin 6 (IL6), an effect completely reversed by a specific inhibitor of TrkA phosphorylation (Fig. 2D, right panel). It is of note that IL6 is related to

Fig. 4. BNN27 differentially regulates TrkA receptor turnover. (**A**) BNN27 facilitated TrkA receptor translocation into membrane lipid rafts. Lipid raft microdomains, marked by the presence of Flotillin-1, were separated from non-raft membrane domains via a sucrose gradient, and analyzed the distribution of TrkA in Control (no ligand), NGF (100 ng/ml) and BNN27 (100 nM) samples after 60 min of exposure using HEK293 cells transfected with a TrkA plasmid. Lysates were subjected to Western blot analysis using specific antibodies against the indicated proteins. Results are representative of three experiments. (**B**) BNN27 *vs* NGF differential regulation of TrkA cell membrane (Biotin): PC12 cells were biotinylated and incubated with NGF (100 ng/ml) or BNN27 (100 nM) for 5, 15 and 30 min. The biotin from the non-internalized proteins was removed using reducing conditions. Surface proteins of cell lysates were precipitated with neutroavidin and subjected to western blot analysis with antibodies against TrkA receptor (upper panel). Positive control (+): total labeled-TrkA at surface. Negative control (−): total TrkA on surfaces with biotin stripped. Lower panel: quantification of internalized TrkA receptor (mean ± SEM, n = 3 experiments, $^*P < 0.05$). (**C**) BNN27 *vs* NGF differential regulation of TrkA cell surface levels (FACS): PC12 cells treated with NGF (100 ng/ml) or BNN27 (100 nM) for 15, 30, 60 or 180 min, surface TrkA receptors stained with anti-TrkA extracellular domain antibodies and exposed to FITC-labeled second antibodies. Surface TrkA receptors were analyzed by flow cytometry (mean ± SEM, n = 3 experiments, $^*P < 0.05$). (**D**) BNN27 *vs* NGF differential regulation of TrkA association to Rab endosomal proteins: PC12 cells were treated with NGF (100 ng/ml) or BNN27 (100 nM) for 15, 30 or 60 min, cells were lysed, immunoprecipitated with TrkA specific antibodies, and immunoblotted with antibodies against Rab5, Rab7, Rab11. Results are representative of three experiments (mean ± SEM, n = 3, $^*P < 0.05$).

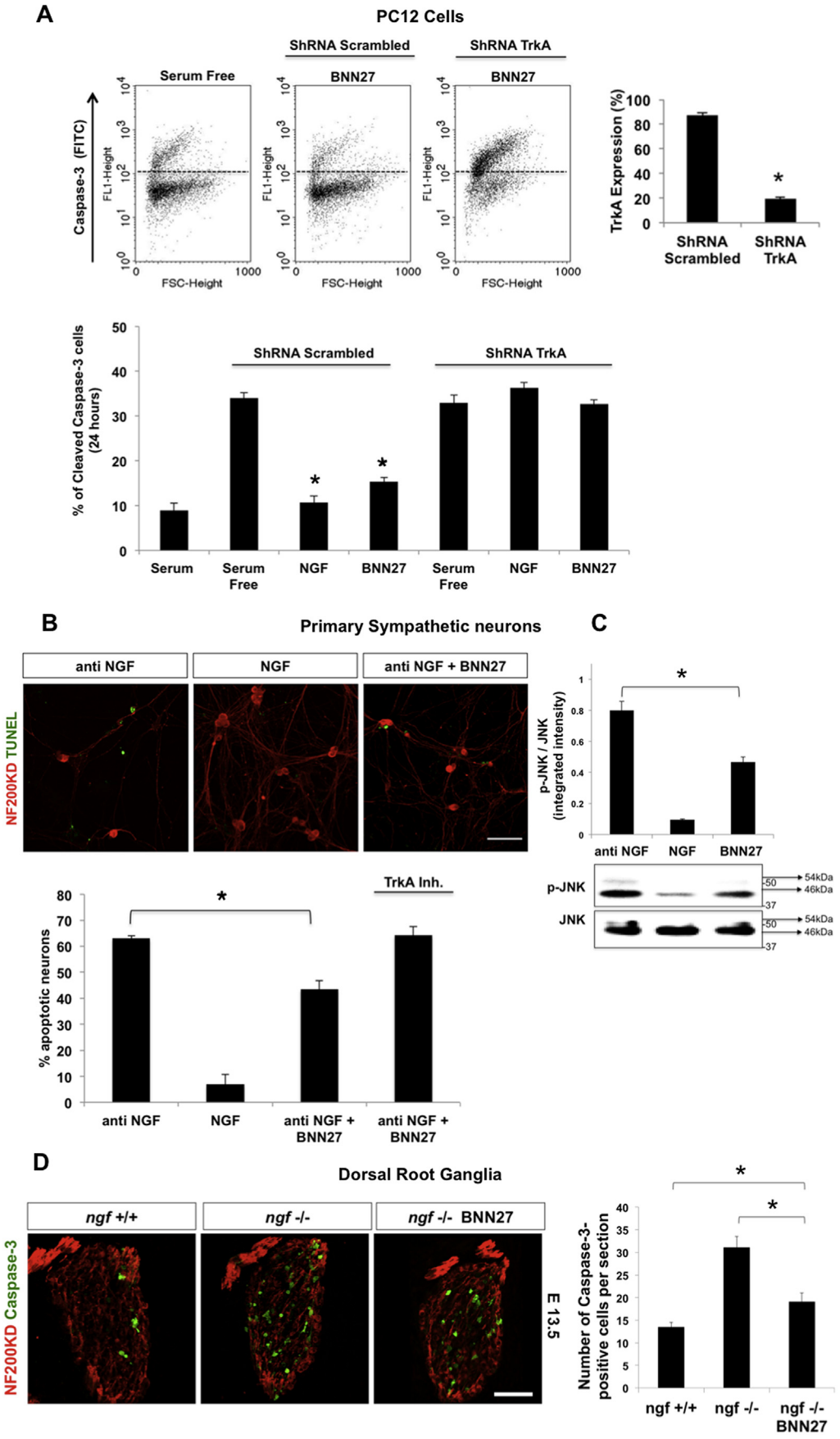
A
PC12 Cells
ShRNA Scrambled
ShRNA TrkA
Serum Free
BNN27
BNN27
Caspase-3 (FITC)
FL1-Height
FSC-Height
TrkA Expression (%)
ShRNA Scrambled
ShRNA TrkA
% of Cleaved Caspase-3 cells (24 hours)
ShRNA Scrambled
ShRNA TrkA
Serum
Serum Free
NGF
BNN27
Serum Free
NGF
BNN27
B
Primary Sympathetic neurons
anti NGF
NGF
anti NGF + BNN27
NF200KD TUNEL
TrkA Inh.
% apoptotic neurons
anti NGF
NGF
anti NGF + BNN27
anti NGF + BNN27
C
p-JNK / JNK (integrated intensity)
anti NGF
NGF
BNN27
p-JNK
JNK
54kDa
46kDa
D
Dorsal Root Ganglia
ngf +/+
ngf -/-
ngf -/- BNN27
NF200KD Caspase-3
E 13.5
Number of Caspase-3-positive cells per section
ngf +/+
ngf -/-
ngf -/- BNN27

CNS diseases where neuroinflammation plays a significant role. Indeed, expression of IL6 is altered in the brain of Alzheimer's disease (AD) patients, specifically increasing around amyloid plaques, and stimulating the synthesis of the AD beta-amyloid precursor protein (Erta et al., 2012).

3.5. BNN27 triggers TrkA activation in a different manner from that of NGF

The BNN27 induction of the phosphorylation of TrkA at tyrosine 490 was dose- and time-dependent, being effective at concentrations as low as 1 nM and reaching plateau at 100 nM (Fig. 3A). Induction of TrkA phosphorylation by BNN27 in CHO cells transfected with the cDNA of the TrkA receptor started within 15 min of its application, and remained up to 6 h, in contrast to the action of NGF, ended within 60 min (Fig. 3B). This observation was further validated in the PC12 cell model. Indeed, BNN27 induced the phosphorylation of TrkA for up to 60 min, while NGF-induced phosphorylation was peaking earlier, at 15 min (Fig. 3C). Interestingly, BNN27 transiently induced ERK1/2 phosphorylation within 30 min, whereas NGF caused a more protracted activation of ERK1/2 reaching 60 min (Fig. 3C).

To further identify the domains of TrkA receptor bound and activated by BNN27, we examined the efficacy of BNN27 in inducing the phosphorylation of the $TrkA^{C302S}$ mutant carrying a point mutation at the cysteine residue 302, which completely abolishes NGF binding (Arevalo et al., 2000). We have found that BNN27, in contrast to NGF, effectively induced the phosphorylation at tyrosine residue 490 in cells transfected with the $TrkA^{C302S}$ mutant (Fig. 3D), suggesting the ability of BNN27 to effectively bind to different binding sites compared to the binding sites of NGF.

In a different set of experiments, we assessed the role of cholesterol-rich membrane lipid rafts in the phosphorylation of TrkA in response to BNN27. Specifically, CHO cells were transfected with a TrkA plasmid and were pretreated with methyl-β-cyclodextrin (MβCD) to extract cholesterol from plasma membranes and to disrupt structure and function of lipid rafts (Limpert et al., 2007). Induction of TrkA phosphorylation by BNN27 was significantly decreased following exposure to MβCD, compared to untreated cells, suggesting that the removal of membrane cholesterol alters the magnitude of TrkA activation by BNN27 (Fig. 3E). It should be noted that cell viability was unaffected by MβCD (data not shown).

3.6. BNN27 differentially regulates TrkA receptor turnover

Although BNN27 binding to TrkA stimulates the phosphorylation of TrkA receptor, BNN27 led to transient activation of the ERK1/2 kinases (Fig. 3C). This discrepancy appears to be due to differences in the selective activation of signaling pathways depending on TrkA receptor enrichment in lipid rafts either at the cell surface or in internal compartments. It has been shown that TrkA receptors in lipid rafts initiate local signaling, whereas, outside lipid rafts, they may activate alternative pathways, possibly involved in retrograde signaling (Tsui-Pierchala et al., 2002; Pike, 2003; Jullien et al., 2002). For this purpose, we focused our attention on the initial step in the cellular compartmentalization of neurotrophin signaling, the focal concentration of Trk receptors within cell surface membrane microdomains.

Specifically, we separated lipid raft microdomains from non-raft membrane domains via a sucrose gradient and analyzed the distribution of TrkA in controls, in NGF-treated and in BNN27-treated samples using $HEK293^{TrkA}$ transfectants. Exposure for 60 min to BNN27 caused the segregation of TrkA into the lipid raft fractions, identified by the presence of Flotillin-1 (Fig. 4A). As a comparison, NGF induced the withdrawal of TrkA receptors from lipid rafts after 60 min of exposure, indicating that TrkA is probably trafficking between the cell surface and diverse intracellular membrane compartments (Fig. 4A).

To assess whether BNN27 mimics NGF in propagating the internalization of TrkA receptor, we used an internalization assay on PC12 cells based on cell surface biotinylation. TrkA quickly internalized after PC12 cells exposure for 15 or 30 min to either NGF or BNN27 (Fig. 4B). We also measured the surface levels of TrkA in non-permeabilized PC12 cells. Levels of TrkA receptors on the cellular surface declined within 30 min of exposure to either NGF or BNN27 (Fig. 4C). Remarkably, there was a significant increase of the surface levels of TrkA in cells exposed for 60 or 180 min to BNN27. However, the levels of TrkA on the surface were decreased in cells exposed to NGF for 60 or 180 min (Fig. 4C).

It is of note that despite the sustained phosphorylation of TrkA receptor by BNN27, the activation of ERK1/2 kinases by BNN27 appears to be transient (Fig. 3C). We used a co-immunoprecipitation method and well-characterized endosomal organelle-specific markers (Jullien et al., 2002): Rab5 (for early endosomes), Rab7 (for late endosomes) and Rab11 (for recycling endosomes) for the evaluation of the kinetics of BNN27-induced TrkA turnover. BNN27 induced the association of TrkA with Rab5 and Rab11 without affecting its association with Rab7 (Fig. 4D). The association of TrkA with Rab11 could explain the observed fast recycling of the receptor back to cell surface (Fig. 4C). It is possible that the apparently protracted binding of TrkA receptor to Rab5 in BNN27-treated cells may be due to the refractoriness of the Rab7-mediated lysosomal processing of the receptor (Fig. 4D). Binding of NGF to the TrkA receptor within endosomes resulted in the maintenance of their signaling capacity (sustained ERK1/2 activation; Fig. 3C), inducing the process of early into late endosomes, ending in lysosomal degradation (Fig. 4D). Our data suggest that BNN27 affects TrkA endocytosis in an apparently dissimilar manner compared to this of NGF.

3.7. BNN27 inhibits apoptosis of NGF-deprived sympathetic neurons through TrkA receptors

We have also examined the involvement of NGF receptors in the anti-apoptotic effects of BNN27 in serum deprived PC12 cells, using shRNAs against the TrkA transcripts. FACS analysis of cells stained

Fig. 5. BNN27 suppressed apoptosis of TrkA-positive neuronal cells. (**A**) shRNA against TrkA receptors reversed the anti-apoptotic effect of BNN27 and NGF on PC12 cells transfected with these shRNAs (mean ± SEM, n = 4 experiments, $^*P < 0.01$, compared to serum free condition). Right panel shows the efficacy of shRNA in suppressing expression of TrkA receptor in PC12 cells, assessed with FACS analysis. (**B**) BNN27 reversed apoptosis of NGF-dependent sympathetic neurons from SCG, isolated from P1 rats. The anti-apoptotic effect of BNN27 was completely blocked by TrkA inhibitor. Neurons were stained with an antibody against NF200kD (red) and with TUNEL (green). More than 300 neurons were counted in six to seven randomly selected optical fields and the percentage of $TUNEL^+$. Scale bar represents 100 μM, (mean ± SEM of apoptotic neurons of n = 6 experiments, $^*P < 0.01$, compared to anti-NGF condition). (**C**) BNN27 attenuates the phosphorylation of JNK in SCG sympathetic neuron cultures after 16 h of NGF withdrawal. Fold change was calculated by densitometric scanning of phospho-JNK signals normalized per total JNK (mean ± SEM, n = 3 experiments, $^*P < 0.01$, compared to anti-NGF condition). (**D**) BNN27 suppressed the apoptotic loss of TrkA positive sensory neurons in dorsal root ganglia of NGF null mouse embryos. Embryos were collected at E13.5 day of pregnancy, sections were stained for apoptotic and neuronal markers: Caspase-3 and NF200kD positive neurons were counted. The results represent the mean ± SEM, n = 3 embryos on each group. Apoptotic neurons per embryo were counted on at least 8 sections from different DRGs. Scale bar represents 75 μM (mean ± SEM, n = 7 experiments, $^*P < 0.05$).

for the apoptotic protein cleaved Caspase-3 revealed that exposure to either BNN27 (100 nM) or NGF (100 ng/ml) reduced the number of apoptotic cells following serum deprivation from 34 ± 1.15% of apoptotic cells (controls) to 15.33 ± 0.88% and 10.66 ± 1.45%, respectively (n = 4, $^*P < 0.01$, compared to serum free condition) (Fig. 5A). Suppression of TrkA expression following exposure of PC12 cells to shRNAs resulted in the almost complete reversal of the anti-apoptotic effects of both NGF and BNN27 (Fig. 5A). The anti-apoptotic effect of NGF and that of BNN27 were also compared using primary sympathetic neurons from P1 rat superior cervical ganglia (SCG). NGF deprivation resulted in a dramatic increase in the number of apoptotic sympathetic neurons (quantified as TUNEL positive cells with condensed nuclei) while this effect was prevented by the addition of 100 nM BNN27 (63 ± 3.6% vs 43 ± 3.2%, n = 6, $^*P < 0.01$, compared to anti-NGF condition; Fig. 5B). Furthermore, the anti-apoptotic effect of BNN27 was significantly reversed in the presence of the selective TrkA inhibitor (64 ± 3.17%, n = 3, $^*P < 0.01$, compared to the action of BNN27 alone), suggesting TrkA receptor as the main mediator of the anti-apoptotic action of BNN27 in sympathetic neurons (Fig. 5B). Finally, NGF deprivation resulted in a dramatic increase of JNK phosphorylation, which was significantly reversed in the presence of either NGF (100 ng/ml) or BNN27 (100 nM). Specifically, JNK activity was decreased about 4.6- and 2-fold in NGF and BNN27 supplementation respectively, compared to anti-NGF control (n = 3, $^*P < 0.01$; Fig. 5C).

3.8. BNN27 reverses apoptosis of TrkA$^+$ sensory neurons in E13.5 NGF null mice embryos

In this set of experiments we have investigated the ability of BNN27 to substitute for NGF in NGF-null mice embryos. It should be noted that in these embryos, TrkA is abundantly expressed in a subpopulation of dorsal root ganglia (DRG) sensory neurons, which have been shown to be entirely dependent on NGF for their survival (Crowley et al., 1994). Indeed, NGF-null mice exhibit a dramatic loss of sensory neurons due to apoptosis on embryonic day 13.5 (E13.5) (White et al., 1996). *ngf*$^{-/-}$ embryos at E14 showed a dramatic increase in the number of Caspase-3 positive neurons in the DRG compared to the *ngf*$^{+/+}$ embryos (Fig. 5D). BNN27 treatment significantly reduced the number of Caspase-3 positive neurons in the DRG to levels comparable to that of *ngf*$^{+/+}$ embryos. (31 ± 2 vs 19 ± 2.3 of Caspase-3 positive neurons per section, n = 6, $^*P < 0.01$).

3.9. Synergistic actions of BNN27 with NGF in neuronal axonal outgrowth

It is well documented that NGF controls the growth of axons in a multitude of neuronal cells including PC12 cells, the classical *in vitro* model to study NGF actions (Greene and Tischler, 1976). There is compelling evidence that the longevity of MAPK activation depends on whether the PC12 cells are stimulated in such a way to either proliferate or to leave cell cycle and proceed into differentiation to neuronal phenotypes (Zhang et al., 2000; Kao et al., 2001; Liu et al., 2007). For this purpose, we compared BNN27 to NGF in their axonal outgrowth effect. Exposure to 100 nM BNN27 did not induce differentiation of PC12 cells into a neuronal phenotype while NGF induced it (Fig. 6A). This difference may be due an inability of BNN27 to keep active the necessary signaling of ERK1/2 kinases. However, BNN27 potentiated the effectiveness of low concentrations of NGF (20 ng/ml instead of the usually effective concentration of 100 ng/ml) in provoking PC12 cell phenotype change from 28 ± 5.6% to 39.6 ± 5.6% (n = 4, $^*P < 0.05$, compared to NGF condition; Fig. 6A) and an increase of maximum neurite length (from 39.6 ± 4 μM to 46.8 ± 5.7 μM (n = 4, $^*P < 0.05$, compared to NGF condition). We have also tested the effect of BNN27 alone or in combination with NGF in rat DRG sensory neurons in culture. 100 nM BNN27 facilitated low concentrations of NGF (20 ng/ml) to increase the axonal length of DRG sensory cells in culture from 99 ± 20 μM to 145 ± 8.9 μM (n = 4, $^*P < 0.05$, compared to NGF condition; Fig. 6B). However, BNN27 alone did not appear to exert any effect on axonal length of primary DRG sensory neurons (data not shown).

3.10. BNN27 does not induce hyperalgesia

Previous studies have shown that NGF induces hyperalgesia and peripheral neuropathic pain (Shu and Mendell, 1999). In order to determine the effect of BNN27 in thermal hyperalgesia in mice under basal conditions, we employed the Hargreaves test. Measurements were taken 30 min following intraplantar or intraperitoneal (i.p.) injection of BNN27 or NGF. As shown in Fig. 7, while intraplantar administration of 1 μg NGF induced a strong hyperalgesic reaction, BNN27, either intraperitoneally (3 mg) or intraplantarily administrated (1 mg), did not alter the thermal nociceptive threshold.

4. Discussion

Our findings provide evidence that the synthetic steroid derivative BNN27 specifically interacts with the TrkA receptor. STD-NMR revealed the binding of BNN27 at the ECDs of the TrkA. Addition of NGF to the TrkA/BNN27 solutions could clarify if the BNN27 binding grooves overlap with the NGF binding epitope at TrkA. Surprisingly, the presence of NGF induced an increase of the BNN27 STD-NMR amplification factor. Since BNN27 does not interact directly with NGF alone, this enhancement possibly reflects the interaction of BNN27 with induced complexes (i.e. 2:2 TrkA:NGF) implying also the formation of new binding site(s). Increasing concentrations of NGF resulted in further enhancement of the STD-NMR amplification factor, which could imply a “positive cooperativity” in the interactions of BNN27 and NGF with the neurotrophin receptors. Molecular dynamic (MD) simulations confirmed the interaction of BNN27 with the TrkA:d5 receptor and moreover highlighted its interaction with contact points of the TrkA-NGF complex, acting as bridge between the two proteins. NGF can facilitate the localization of TrkA receptors within the lipid rafts, however it phosphorylates TrkA receptors localized both in the lipid raft and non-raft domains of the membrane (Pryor et al., 2012; Limpert et al., 2007). On the contrary, our data show that BNN27 phosphorylates TrkA receptors only within the lipid rafts. Indeed, depletion of lipid rafts by methyl-β-cyclodextrin (MβCD), results in the loss of the efficacy of BNN27 to phosphorylate TrkA receptors. The highly lipophilic, steroidal nature of BNN27 may also contribute in this phenomenon, related to membrane fluidity and micro-organization. It is of note that despite the sustained phosphorylation of TrkA receptor, BNN27 activates the ERK1/2 kinases only in a transient manner in contrast to NGF. These findings suggest that BNN27-mediated activation of the TrkA receptor is resulting in different intracellular signaling pathways.

Interestingly, various endogenous steroids and the synthetic steroid analog BNN27, exert structure-dependent, differential effects on neurotrophin receptor activation. Indeed, DHEA binds to all three Trk receptors (TrkA, TrkB, TrkC), induces tyrosine phosphorylation of TrkA and TrkC receptors but does not appear to affect the phosphorylation of TrkB receptors (Pediaditakis et al., 2015). Estradiol does not interact with and directly affect neurotrophin receptors and DHEA first metabolite, ADIOL, shows no affinity for TrkA receptors, while BNN27 binds to and activates TrkA but not TrkB or TrkC receptors. Thus, it appears that the structural and stereo-chemical characteristics of a steroid and especially the

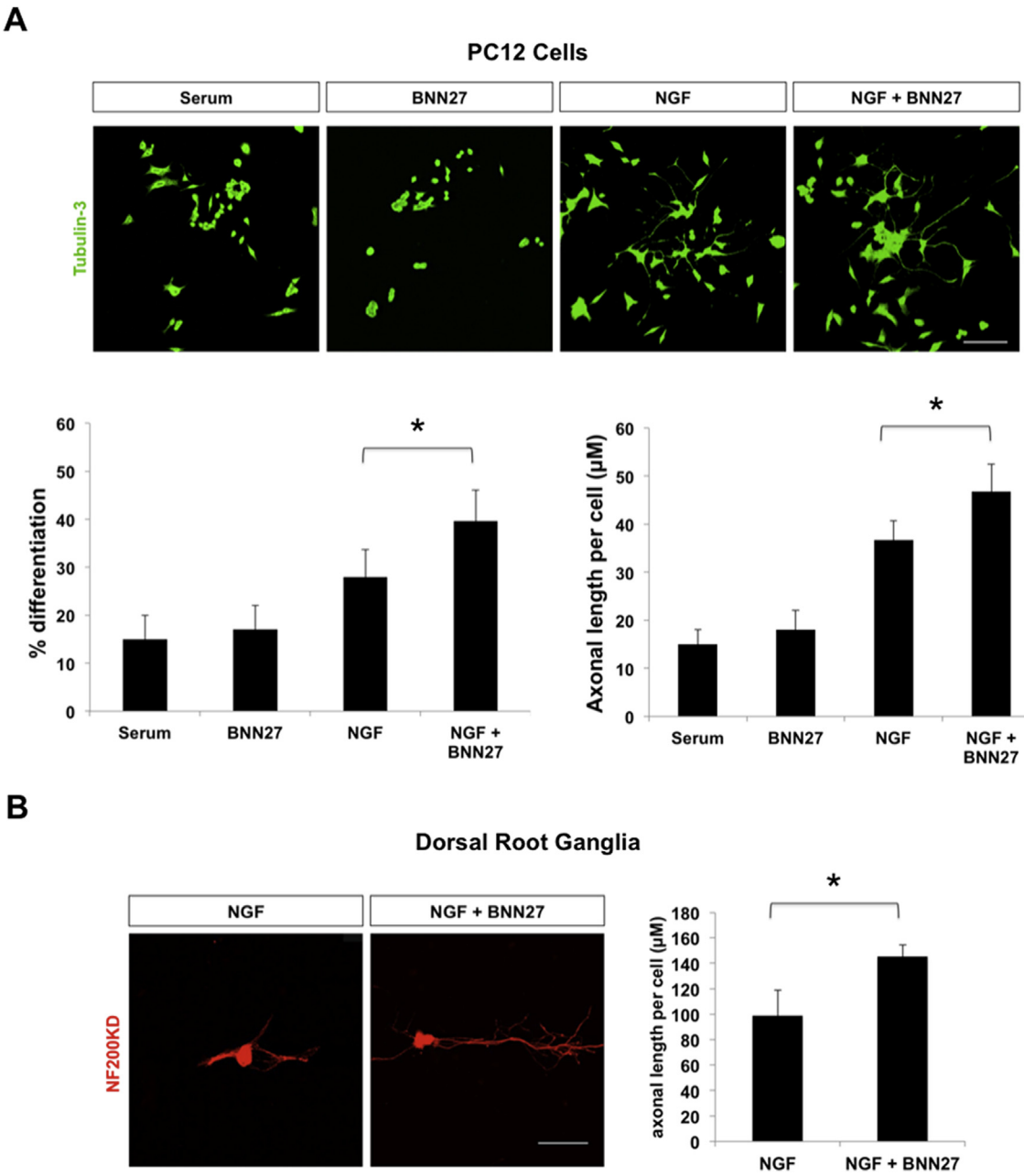

Fig. 6. BNN27 facilitated the effects of NGF on neurite outgrowth. (**A**) PC12 cells or (**B**) sensory neurons of dissociated rat DRGs were incubated for 24 h with NGF (20 ng/ml) in the absence or the presence of BNN27 (100 nM) and stained with antibodies against Tubulin-3 in PC12 cells or NF200kD in sensory neurons. Results are expressed as mean percentage of cells having neurites longer than their soma. The length of each neurite from at least 50 cells in 4 optical fields in each condition was counted in n = 4 experiments, $^{*}P < 0.05$, compared to NGF condition.

substitution pattern at C17 of the 5-androstene skeleton determines binding and activation efficacy of TrkA receptors, as in the case of classical steroid receptors.

BNN27 shows a spectacular specificity and affinity towards the TrkA receptor compared to other small molecules, reported to also interact with this receptor. Indeed, gambogic amide was shown to bind with low affinity to the cytoplasmic juxta-membrane domain of TrkA, but not TrkB or TrkC, inducing TrkA tyrosine phosphorylation and the downstream signaling activation, including AKT and MAPKs (Jang et al., 2007). Amitriptyline interacts also with the extracellular domain of TrkB receptor (Jang et al., 2009). Recently, TrkA and TrkB low affinity agonists (compounds MT2 and LM22A respectively) have also been reported, using *in silico* screening, to specifically activate these receptors (Scarpi et al., 2012; Massa et al., 2010).

Intracellular trafficking of TrkA receptor in response to NGF is of critical importance in neurotrophic activity (Yu et al., 2011; Kuruvilla et al., 2004). Recent studies have highlighted abnormalities in TrkA intracellular trafficking in several neurodegenerative diseases, including Alzheimer's (Millecamps and Julien, 2013). Our data show that BNN27 induces a different pattern of TrkA turnover compared to that of NGF. More specifically, BNN27 facilitates an internalization and fast translocation of the receptor back to cell surface through the persistent association of Rab5 with TrkA receptor, docking of the receptor in the recycling endosomes (Rab11) and blocking the interaction of TrkA with the late endosomes

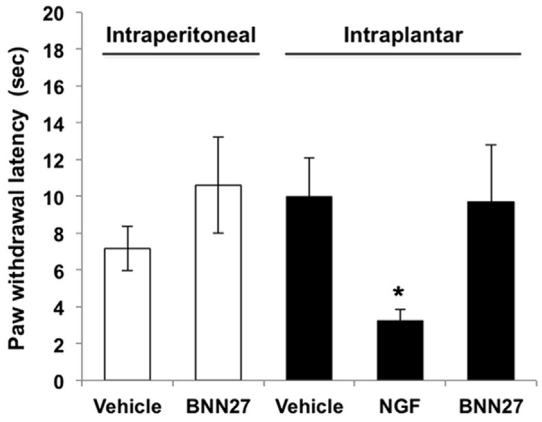

Fig. 7. BNN27 suppressed thermal hyperalgesia. To evaluate the effect of BNN27 in thermal hyperalgesia in mice under basal conditions, we used the Hargreaves test. Measurements were taken 30 min following intraplantar or intraperitoneal (i.p.) injection of BNN27 or NGF (mean ± SEM, n = 7 experiments, $^{*}P < 0.05$).

(Rab7) and thus the maintenance of their signaling capacity (Fig. 8).

It is of interest that neuronal differentiation is promoted by activated TrkA receptors within the endosomes (signaling endosomes) sustaining activation of the kinase ERK1/2 (Zhang et al., 2000; Kao et al., 2001; Liu et al., 2007). In our hands, BNN27 does not appear to induce the differentiation of PC12 cells into a neuronal phenotype and this may be due an inability of BNN27 to sustain the necessary signaling of ERK1/2 kinases. However, BNN27 secures higher levels of surface TrkA, inducing its faster recycling into the membranes, and potentiating the effects of low concentrations of NGF in axonal growth sprouting. BNN27 was also shown to be ineffective in inducing differentiation and neurite outgrowth of mouse sensory neurons in culture. However, when it was combined with low concentrations of NGF it significantly increased the efficacy of the latter in inducing the percentage of enhanced axonal length in both cell systems (as summarized in Fig. 8). These data suggest that the combination of BNN27 and NGF will act in parallel by the BNN27-driven fast returning of the internalized TrkA receptor in the membrane through early endosomes, increasing thus the levels of functional TrkA receptors occupied by NGF which afterwards induce full late endocytosis signaling of the NGF-TrkA complex, enhancing neurite outgrowth. This possibility is of particular pharmacological interest, since lower levels of NGF have been reported in Alzheimer's disease (Matrone et al., 2008). Since BNN27 shows not full capacity to support a complete endosomal TrkA processing from early to late endosomes, its effectiveness alone in initiating neurite outgrowth and axonal extension is limited.

BNN27 effectively mimicked NGF in inhibiting serum deprivation- or NGF withdrawal-driven apoptosis of various NGF-dependent neuronal cell types, an effect that is mediated by TrkA receptors. Furthermore, BNN27 appears to rescue from apoptosis TrkA-positive sensory neurons of Dorsal Root Ganglia (DRG) in *ngf*$^{-/-}$ mouse embryos at the age of E13.5, at the time of naturally occurring programmed cell death (White et al., 1996). These findings suggest that derivative BNN27 acts as a synthetic

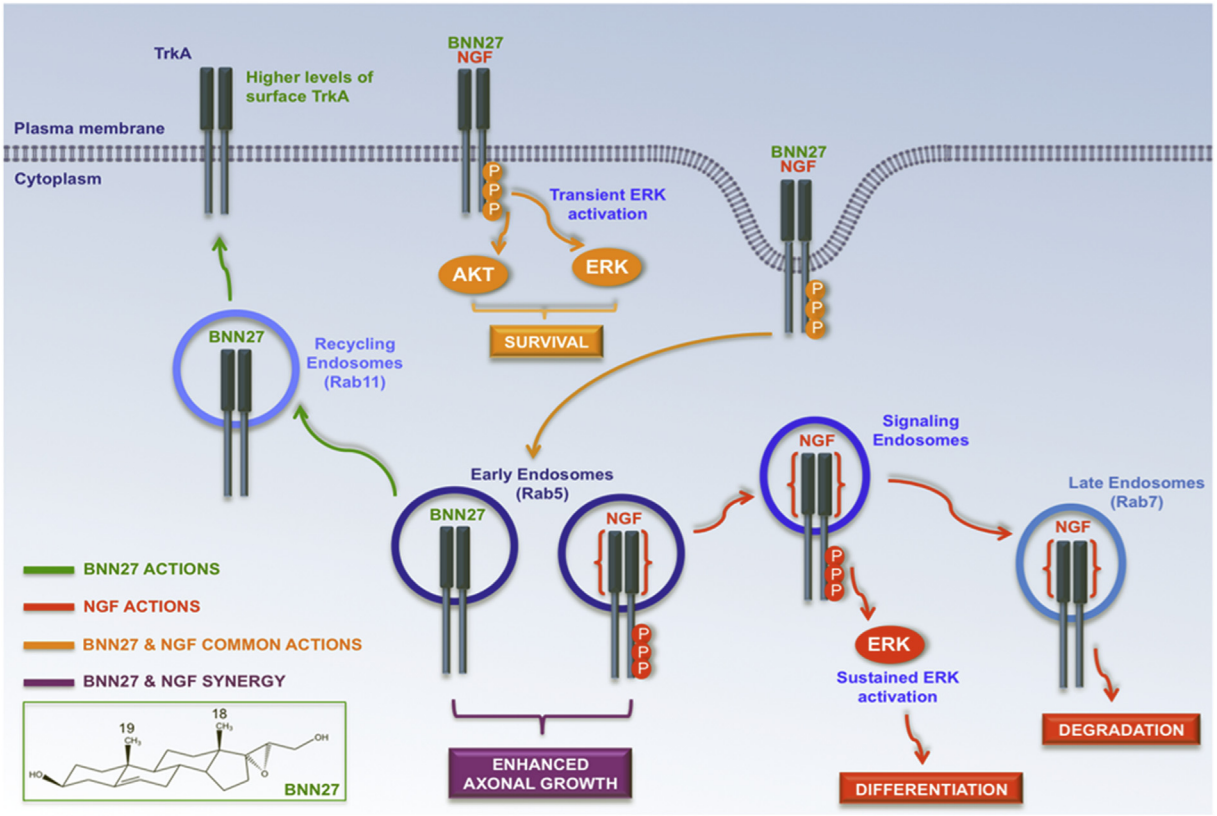

Fig. 8. Schematic representation of the actions of BNN27 on TrkA receptor signaling and turnover. BNN27 specifically interacts with TrkA receptor at nanomolar concentrations and induces TrkA tyrosine phosphorylation, affecting downstream signaling of ERK and AKT in a different time pattern than that of NGF. BNN27 induces internalization and fast return of the receptor into the membrane through activation of Rab5 protein, docking the receptor in early/recycling endosomes. In contrast, NGF-activated TrkA receptors maintained their signaling capacity and trafficking from early into late endosomes, ending in lysosomal degradation. BNN27 exerts strong anti-apoptotic, neuroprotective actions via NGF receptors and potentiates the effects of NGF in the induction of neurite elongation.

microneurotrophin agonist.

A growing number of published experimental and clinical protocols evaluating the utilization of NGF in the armamentarium against neurodegenerative diseases both as preventive or therapeutic agent acting as neural tissue protector and/or repairer of neuronal deficits (Calissano et al., 2010; Matrone et al., 2008). Our data suggest that BNN27 mimics some of the neuroprotective effects of NGF (designated as a synthetic microneurotrophin). It is of particular note that BNN27 does not reproduce *in vivo* the problematic hyperalgesic effects of NGF (Shu and Mendell, 1999). Synthetic compounds like BNN27 may serve as lead molecules to develop brain-permeable small agonists or antagonists of neurotrophin receptors with selective neuroprotective and neurogenic actions and potential applications in therapeutics of neurodegenerative diseases and brain trauma. In addition, these molecules provide a powerful tool for dissecting and studying the multiple signaling pathways of neurotrophin receptors and their importance in cell death prevention and neuronal differentiation.

Authors' contribution

A.G. and I.C. conceived and supervised the project. A.G., I.C., T.C. and I.P. designed the experiments, interpreted data, drafted and revised the manuscript. I.P. performed most of the experiments and analyzed the data. P.E. performed the experiments on $ngf^{-/-}$ mice and experimented with primary neuronal cultures. K.C.P., M.Z., C.P. and T.C. contributed to the synthesis of immobilized BNN27, molecular modeling studies and STD NMR experiments. J.C.A. performed the surface biotinylation assays. V.N. and N.T. designed, performed and analyzed the experiments for lipid rafts fractionation. V.I.A. and T.Ch. designed and carried out microglia experiments. E.K. and M.V. conducted pain experiments and analyzed the data. A.N.M. helped with data analysis and writing of the manuscript. All authors approved the version that was submitted.

Conflict of interest statement

All authors, except Achille Gravanis, declare that they have not any competing financial interests in relation to the work described. Dr Achille Gravanis is the co-founder of spin-off Bionature EA LTD, proprietary of compound BNN27 (patented with the WO 2008/1555 34 A2 number at the World Intellectual Property Organization).

Acknowledgments

Funded by the ERC01 National Initiative grant, General Secretariat for Research Technology, partially supported by Bionature E.A. Ltd and Bodossaki Foundation.

Appendix A. Supplementary data

Supplementary data related to this article can be found at http://dx.doi.org/10.1016/j.neuropharm.2016.09.007.

References

Arevalo, J.C., Conde, B., Hempstead, B.L., Chao, M.V., Martin-Zanca, D., Perez, P., 2000. TrkA immunoglobulin-like ligand binding domains inhibit spontaneous activation of the receptor. Mol. Cell Biol. 20, 5908–5916.
Bibel, M., Barde, Y.A., 2000. Neurotrophins: key regulators of cell fate and cell shape in the vertebrate nervous system. Genes Dev. 14, 2919–2937.
Calissano, P., Matrone, C., Amadoro, G., 2010. Nerve growth factor as a paradigm of neurotrophins related to Alzheimer's disease. Dev. Neurobiol. 70, 372–383.
Calogeropoulou, T., Avlonitis, N., Minas, V., Alexi, X., Pantzou, A., Charalampopoulos, I., Zervou, M., Vergou, V., Katsanou, E.S., Lazaridis, I., Alexis, M.N., Gravanis, A., 2009. Novel dehydroepiandrosterone derivatives with antiapoptotic, neuroprotective activity. J. Med. Chem. 52, 6569–6587.
Charalampopoulos, I., Remboutsika, E., Margioris, A.N., Gravanis, A., 2008. Neurosteroids as modulators of neurogenesis and neuronal survival. Trends Endocrinol. Metab. 19, 300–307.
Charalampopoulos, I., Tsatsanis, C., Dermitzaki, E., Alexaki, V.I., Castanas, E., Margioris, A.N., Gravanis, A., 2004. Dehydroepiandrosterone and allopregnanolone protect sympathoadrenal medulla cells against apoptosis via anti-apoptotic Bcl-2 proteins. Proc. Natl. Acad. Sci. U. S. A. 101, 8209–8214.
Covaceuszach, S., Capsoni, S., Ugolini, G., Spirito, F., Vignone, D., Cattaneo, A., 2009. Development of a non invasive NGF-based therapy for Alzheimer's disease. Curr. Alzheimer Res. 6, 158–170.
Crowley, C., Spencer, S.D., Nishimura, M.C., Chen, K.S., Pitts-Meek, S., Armanini, M.P., Ling, L.H., McMahon, S.B., Shelton, D.L., Levinson, A.D., et al., 1994. Mice lacking nerve growth factor display perinatal loss of sensory and sympathetic neurons yet develop basal forebrain cholinergic neurons. Cell 76, 1001–1011.
Eriksdotter Jonhagen, M., Nordberg, A., Amberla, K., Backman, L., Ebendal, T., Meyerson, B., Olson, L., Seiger, Shigeta, M., Theodorsson, E., Viitanen, M., Winblad, B., Wahlund, L.O., 1998. Intracerebroventricular infusion of nerve growth factor in three patients with Alzheimer's disease. Dement. Geriatr. Cogn. Disord. 9, 246–257.
Erta, M., Quintana, A., Hidalgo, J., 2012. Interleukin-6, a major cytokine in the central nervous system. Int. J. Biol. Sci. 8, 1254–1266.
Greene, L.A., Tischler, A.S., 1976. Establishment of a noradrenergic clonal line of rat adrenal pheochromocytoma cells which respond to nerve growth factor. Proc. Natl. Acad. Sci. U. S. A. 73, 2424–2428.
Hargreaves, K., Dubner, R., Brown, F., Flores, C., Joris, J., 1988. A new and sensitive method for measuring thermal nociception in cutaneous hyperalgesia. Pain 32, 77–88.
Jang, S.W., Liu, X., Chan, C.B., Weinshenker, D., Hall, R.A., Xiao, G., Ye, K., 2009. Amitriptyline is a TrkA and TrkB receptor agonist that promotes TrkA/TrkB heterodimerization and has potent neurotrophic activity. Chem. Biol. 16, 644–656.
Jang, S.W., Okada, M., Sayeed, I., Xiao, G., Stein, D., Jin, P., Ye, K., 2007. Gambogic amide, a selective agonist for TrkA receptor that possesses robust neurotrophic activity, prevents neuronal cell death. Proc. Natl. Acad. Sci. U. S. A. 104, 16329–16334.
Jullien, J., Guili, V., Reichardt, L.F., Rudkin, B.B., 2002. Molecular kinetics of nerve growth factor receptor trafficking and activation. J. Biol. Chem. 277, 38700–38708.
Kao, S., Jaiswal, R.K., Kolch, W., Landreth, G.E., 2001. Identification of the mechanisms regulating the differential activation of the mapk cascade by epidermal growth factor and nerve growth factor in PC12 cells. J. Biol. Chem. 276, 18169–18177.
Kaplan, D.R., Miller, F.D., 2000. Neurotrophin signal transduction in the nervous system. Curr. Opin. Neurobiol. 10, 381–391.
Kuruvilla, R., Zweifel, L.S., Glebova, N.O., Lonze, B.E., Valdez, G., Ye, H., Ginty, D.D., 2004. A neurotrophin signaling cascade coordinates sympathetic neuron development through differential control of TrkA trafficking and retrograde signaling. Cell 118, 243–255.
Lazaridis, I., Charalampopoulos, I., Alexaki, V.I., Avlonitis, N., Pediaditakis, I., Efstathopoulos, P., Calogeropoulou, T., Castanas, E., Gravanis, A., 2011. Neurosteroid dehydroepiandrosterone interacts with nerve growth factor (NGF) receptors, preventing neuronal apoptosis. Plos Biol. 9, e1001051.
Limpert, A.S., Karlo, J.C., Landreth, G.E., 2007. Nerve growth factor stimulates the concentration of TrkA within lipid rafts and extracellular signal-regulated kinase activation through c-Cbl-associated protein. Mol. Cell Biol. 27, 5686–5698.
Liu, J., Lamb, D., Chou, M.M., Liu, Y.J., Li, G., 2007. Nerve growth factor-mediated neurite outgrowth via regulation of Rab5. Mol. Biol. Cell 18, 1375–1384.
Massa, S.M., Yang, T., Xie, Y., Shi, J., Bilgen, M., Joyce, J.N., Nehama, D., Rajadas, J., Longo, F.M., 2010. Small molecule BDNF mimetics activate TrkB signaling and prevent neuronal degeneration in rodents. J. Clin. Investig. 120, 1774–1785.
Matrone, C., Ciotti, M.T., Mercanti, D., Marolda, R., Calissano, P., 2008. NGF and BDNF signaling control amyloidogenic route and Abeta production in hippocampal neurons. Proc. Natl. Acad. Sci. U. S. A. 105, 13139–13144.
Mayer, M., Meyer, B., 1999. Characterization of ligand binding by saturation transfer difference NMR spectroscopy. Angew. Chem. Int. Ed. Engl. 38, 1784–1788.
Meyer, B., Peters, T., 2003. NMR spectroscopy techniques for screening and identifying ligand binding to protein receptors. Angew. Chem. Int. Ed. Engl. 42, 864–890.
Millecamps, S., Julien, J.P., 2013. Axonal transport deficits and neurodegenerative diseases. Nat. Rev. Neurosci. 14, 161–176.
Miller, K.K., Al-Rayyan, N., Ivanova, M.M., Mattingly, K.A., Ripp, S.L., Klinge, C.M., Prough, R.A., 2013. DHEA metabolites activate estrogen receptors alpha and beta. Steroids 78, 15–25.
Nikoletopoulou, V., Lickert, H., Frade, J.M., Rencurel, C., Giallonardo, P., Zhang, L., Bibel, M., Barde, Y.A., 2010. Neurotrophin receptors TrkA and TrkC cause neuronal death whereas TrkB does not. Nature 467, 59–63.
Pediaditakis, I., Iliopoulos, I., Theologidis, I., Delivanoglou, N., Margioris, A.N., Charalampopoulos, I., Gravanis, A., 2015. Dehydroepiandrosterone: an ancestral ligand of neurotrophin receptors. Endocrinology 156, 16–23.
Pike, L.J., 2003. Lipid rafts: bringing order to chaos. J. Lipid Res. 44, 655–667.
Pryor, S., McCaffrey, G., Young, L.R., Grimes, M.L., 2012. NGF causes TrkA to specifically attract microtubules to lipid rafts. Plos One 7, e35163.
Rossner, S., Ueberham, U., Schliebs, R., Perez-Polo, J.R., Bigl, V., 1998. The regulation of amyloid precursor protein metabolism by cholinergic mechanisms and

neurotrophin receptor signaling. Prog. Neurobiol. 56, 541–569.
Scarpi, D., Cirelli, D., Matrone, C., Castronovo, G., Rosini, P., Occhiato, E.G., Romano, F., Bartali, L., Clemente, A.M., Bottegoni, G., Cavalli, A., De Chiara, G., Bonini, P., Calissano, P., Palamara, A.T., Garaci, E., Torcia, M.G., Guarna, A., Cozzolino, F., 2012. Low molecular weight, non-peptidic agonists of TrkA receptor with NGF-mimetic activity. Cell Death Dis. 3, e339.
Shu, X.Q., Mendell, L.M., 1999. Neurotrophins and hyperalgesia. Proc. Natl. Acad. Sci. U. S. A. 96, 7693–7696.
Teng, H.K., Teng, K.K., Lee, R., Wright, S., Tevar, S., Almeida, R.D., Kermani, P., Torkin, R., Chen, Z.Y., Lee, F.S., Kraemer, R.T., Nykjaer, A., Hempstead, B.L., 2005. ProBDNF induces neuronal apoptosis via activation of a receptor complex of p75NTR and sortilin. J. Neurosci. 25, 5455–5463.
Tian, L., Guo, R., Yue, X., Lv, Q., Ye, X., Wang, Z., Chen, Z., Wu, B., Xu, G., Liu, X., 2012. Intranasal administration of nerve growth factor ameliorate beta-amyloid deposition after traumatic brain injury in rats. Brain Res. 1440, 47–55.
Tsui-Pierchala, B.A., Encinas, M., Milbrandt, J., Johnson Jr., E.M., 2002. Lipid rafts in neuronal signaling and function. Trends Neurosci. 25, 412–417.
Tuszynski, M.H., Thal, L., Pay, M., Salmon, D.P., U, H.S., Bakay, R., Patel, P., Blesch, A., Vahlsing, H.L., Ho, G., Tong, G., Potkin, S.G., Fallon, J., Hansen, L., Mufson, E.J., Kordower, J.H., Gall, C., Conner, J., 2005. A phase 1 clinical trial of nerve growth factor gene therapy for Alzheimer disease. Nat. Med. 11, 551–555.
Tuszynski, M.H., Yang, J.H., Barba, D., U, H.S., Bakay, R.A., Pay, M.M., Masliah, E., Conner, J.M., Kobalka, P., Roy, S., Nagahara, A.H., 2015. Nerve growth factor gene therapy: activation of neuronal responses in Alzheimer disease. JAMA Neurol. 72 (10), 1139–1147.
White, F.A., Silos-Santiago, I., Molliver, D.C., Nishimura, M., Phillips, H., Barbacid, M., Snider, W.D., 1996. Synchronous onset of NGF and TrkA survival dependence in developing dorsal root ganglia. J. Neurosci. 16, 4662–4672.
Wiesmann, C., Ultsch, M.H., Bass, S.H., de Vos, A.M., 1999. Crystal structure of nerve growth factor in complex with the ligand-binding domain of the TrkA receptor. Nature 401, 184–188.
Yu, T., Calvo, L., Anta, B., Lopez-Benito, S., Southon, E., Chao, M.V., Tessarollo, L., Arevalo, J.C., 2011. Regulation of trafficking of activated TrkA is critical for NGF-mediated functions. Traffic 12, 521–534.
Yuan, J., Yankner, B.A., 2000. Apoptosis in the nervous system. Nature 407, 802–809.
Zhang, Y., Moheban, D.B., Conway, B.R., Bhattacharyya, A., Segal, R.A., 2000. Cell surface Trk receptors mediate NGF-induced survival while internalized receptors regulate NGF-induced differentiation. J. Neurosci. 20, 5671–5678.
Zhang, Z.H., Xi, G.M., Li, W.C., Ling, H.Y., Qu, P., Fang, X.B., 2010. Cyclic-AMP response element binding protein and tau are involved in the neuroprotective mechanisms of nerve growth factor during focal cerebral ischemia/reperfusion in rats. J. Clin. Neurosci. 17, 353–356.